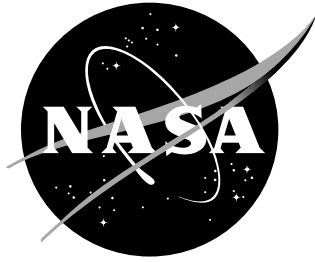


NASA/TM-1999-208972



Effective Thermal Conductivity of High Temperature Insulations for Reusable Launch Vehicles

Kamran Daryabeigi
Langley Research Center, Hampton, Virginia

February 1999

The NASA STI Program Office ... in Profile

Since its founding, NASA has been dedicated to the advancement of aeronautics and space science. The NASA Scientific and Technical Information (STI) Program Office plays a key part in helping NASA maintain this important role.

The NASA STI Program Office is operated by Langley Research Center, the lead center for NASA's scientific and technical information. The NASA STI Program Office provides access to the NASA STI Database, the largest collection of aeronautical and space science STI in the world. The Program Office is also NASA's institutional mechanism for disseminating the results of its research and development activities. These results are published by NASA in the NASA STI Report Series, which includes the following report types:

- **TECHNICAL PUBLICATION.** Reports of completed research or a major significant phase of research that present the results of NASA programs and include extensive data or theoretical analysis. Includes compilations of significant scientific and technical data and information deemed to be of continuing reference value. NASA counterpart of peer-reviewed formal professional papers, but having less stringent limitations on manuscript length and extent of graphic presentations.
- **TECHNICAL MEMORANDUM.** Scientific and technical findings that are preliminary or of specialized interest, e.g., quick release reports, working papers, and bibliographies that contain minimal annotation. Does not contain extensive analysis.
- **CONTRACTOR REPORT.** Scientific and technical findings by NASA-sponsored contractors and grantees.

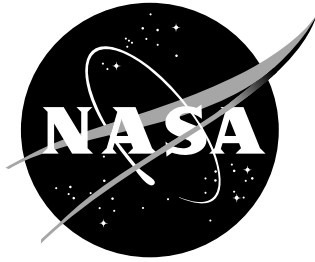
- **CONFERENCE PUBLICATION.** Collected papers from scientific and technical conferences, symposia, seminars, or other meetings sponsored or co-sponsored by NASA.
- **SPECIAL PUBLICATION.** Scientific, technical, or historical information from NASA programs, projects, and missions, often concerned with subjects having substantial public interest.
- **TECHNICAL TRANSLATION.** English-language translations of foreign scientific and technical material pertinent to NASA's mission.

Specialized services that complement the STI Program Office's diverse offerings include creating custom thesauri, building customized databases, organizing and publishing research results ... even providing videos.

For more information about the NASA STI Program Office, see the following:

- Access the NASA STI Program Home Page at <http://www.sti.nasa.gov>
- E-mail your question via the Internet to help@sti.nasa.gov
- Fax your question to the NASA STI Help Desk at (301) 621-0134
- Phone the NASA STI Help Desk at (301) 621-0390
- Write to:
NASA STI Help Desk
NASA Center for AeroSpace Information
7121 Standard Drive
Hanover, MD 21076-1320

NASA/TM-1999-208972



Effective Thermal Conductivity of High Temperature Insulations for Reusable Launch Vehicles

Kamran Daryabeigi
Langley Research Center, Hampton, Virginia

National Aeronautics and
Space Administration

Langley Research Center
Hampton, Virginia 23681-2199

February 1999

Acknowledgments

The author gratefully acknowledges the contributions of Wayne D. Geouge and Jeffrey R. Knutson of NASA Langley Research Center, Hampton, Virginia.

The use of trademarks or names of manufacturers in the report is for accurate reporting and does not constitute an official endorsement, either expressed or implied, of such products or manufacturers by the National Aeronautics and Space Administration.

Available from:

NASA Center for AeroSpace Information (CASI)
7121 Standard Drive
Hanover, MD 21076-1320
(301) 621-0390

National Technical Information Service (NTIS)
5285 Port Royal Road
Springfield, VA 22161-2171
(703) 605-6000

Abstract

An experimental apparatus was designed to measure the effective thermal conductivity of various high temperature insulations subject to large temperature gradients representative of typical launch vehicle re-entry aerodynamic heating conditions. The insulation sample cold side was maintained around room temperature, while the hot side was heated to temperatures as high as 1800°F. The environmental pressure was varied from 1×10^{-4} to 760 torr. All the measurements were performed in a dry gaseous nitrogen environment. The effective thermal conductivity of the following insulation samples were measured: Saffil™ at 1.5, 3, 6 lb/ft³, Q-Fiber™ felt at 3, 6 lb/ft³, Cerachrome™ at 6, 12 lb/ft³, and three multi-layer insulation configurations at 1.5 and 3 lb/ft³.

Introduction

Metallic and refractory-composite thermal protection systems are being considered for a new generation of reusable launch vehicles (RLV). The main function of the thermal protection system (TPS) is to maintain the vehicle structural temperature within acceptable limits during re-entry aerodynamic heating. The metallic TPS consists of a metallic shell panel fabricated from high temperature metallic alloy and mechanically attached to the substructure. The refractory-composite TPS consists of a composite shell panel. In either case, the shell is filled with lightweight, non load-bearing, high-temperature fibrous insulation. Insulation for current metallic TPS for RLV experiences environmental pressures from 1×10^{-4} to 760 torr, while the hot surface of insulation is exposed to temperatures as high as 1800°F.

Heat transfer through the insulation involves combined modes of heat transfer: solid conduction through fibers, gas conduction and natural convection in the space between fibers, and radiation through participating media which includes absorption, scattering and emission of radiant energy by the fibers. The relative contributions of the different heat transfer modes vary during re-entry. Radiation becomes more dominant at high temperatures with large temperature differences through the insulation, while gas conduction and natural convection contributions are minimal at low pressures and become more significant with increasing pressure. The complex coupling of the heat transfer modes makes the analysis and design of high-temperature insulation difficult.

Heat transfer through insulation for re-entry aerodynamic heating is a transient problem, and both the thermal conductivity and specific heat of insulation as a function of temperature and pressure are required for complete analysis. As a first step, the steady-state performance of the insulation should be characterized by measuring the effective thermal conductivity of the insulation, where the contributions of various modes of heat transfer are lumped in to an effective thermal conductivity. The experimental apparatus for measuring the effective thermal conductivity shall be capable of providing thermal conductivity measurements at conditions representative of re-entry aerodynamic heating conditions for RLV. This means measuring thermal conductivity at environmental pressures from 10^{-4} to 760 torr, and at temperatures from room temperature up to 1800°F. Because radiation through participating media is an important component of heat transfer through insulation having large temperature gradients, the apparatus should be capable of imposing temperature differences through the sample as high as 1800°F. The American Society for Testing and Materials (ASTM) standard C-201¹ entitled "Standard Test Method for Thermal Conductivity of Refractories" meets the requirements for this investigation. Therefore, a thermal conductivity apparatus was designed and fabricated that closely resembled this

ASTM standard. The apparatus can be easily modified to measure the transient performance of the insulation.

The overall objective of this study is to design an experimental apparatus for measuring the effective thermal conductivity of high-temperature insulations, and to compare the effective thermal conductivity of four high-temperature insulations.

Thermal Conductivity Apparatus

The apparatus used in this study followed the general guidelines from ASTM standard C-201¹. The standard consists of a radiant heater, a silicon carbide septum plate directly placed on the specimen to provide a flat boundary and a uniform hot-face temperature, and a water-cooled plate containing three water calorimeters. The water calorimeters are maintained at 80.6°F (27 °C) while the hot surface can be heated to temperatures as high as 2732°F (1500°C). The main components of the thermal conductivity apparatus used in the present study consist of a radiant heater, an Inconel™ Alloy septum plate directly placed on the specimen to provide a flat, uniform temperature boundary, and a water-cooled plate containing thin film heat flux gages. A schematic of the apparatus is shown in Figure 1. The main difference between this apparatus and the ASTM standard is that thin foil heat flux gages are used for measuring the heat flux in the present apparatus, while water calorimeters are used in the ASTM standard.

The apparatus consists of a water-cooled plate made of aluminum, 12 × 12 × 1 inches, with seven coolant passages across the length of the plate. Each coolant passage is 0.375 inches in diameter, and centered along the plate thickness. A polyimide sheet 0.005 inches thick is bonded to the top of the water-cooled plate. The top side of the polyimide sheet constitutes the “cold side” boundary for the insulation. A picture frame made of refractory ceramic board is set on the water-cooled plate to provide support for the septum plate. The insulation sample to be tested is placed inside the picture frame. The ceramic board picture frame is two inches wide and its outside dimensions are 12 × 12 inches resulting in a test sample size of eight by eight inches. The ceramic board picture frame’s thickness can vary between 0.5 and 2 inches. For the tests reported in the present study, the ceramic board picture frame and thus the insulation sample is 0.522 inches thick. A photograph of the water-cooled plate with the ceramic board picture frame set on top of the plate is shown in Figure 2.

A septum plate made of Inconel™ alloy 625, with dimensions of 12 × 12 × ¼ inches is used to provide a uniform temperature boundary for the test specimen. The septum plate is placed directly on top of the picture frame and the insulation sample. The bottom of the septum plate constitutes the “hot side” boundary for the insulation sample. To alleviate bowing of the septum plate due to temperature gradients from the plate center to plate edges, a series of slots 1.5 inches long, 0.060 inches wide were made around the circumference of the plate with one-inch spacing, as shown in Figure 3

The apparatus uses a commercially available ceramic-fiber radiant heater which consists of rows of iron-chrome-aluminum heater wires cast in a two inch thick ceramic, such that the heating elements are located near the front surface. The heater is 12 × 12 inches and is encased in a 2.5 inch deep sheet metal case with ceramic fiber insulation on the backside of the heating elements. The heater surface can be heated up to 2000°F. The heater is located approximately 1.5 inches above the septum plate. The whole assembly is insulated with one-inch thick refractory ceramic board, as shown in Figure 4, with additional insulation set on top of the heater, to minimize heat losses. The apparatus is placed in a 5 feet diameter, 5 feet long vacuum chamber capable of providing test pressures from 1×10^{-4} to 760 torr. A photograph of the apparatus in the vacuum chamber is shown in Figure 5.

For all the tests reported in the present study, the insulation sample was sandwiched between two parallel horizontal plates oriented perpendicular to local gravity vector. The lower plate (water-cooled plate) has a lower temperature than the upper plate (septum plate), therefore, eliminating natural convection heat transfer through the insulation. The only heat transfer mechanisms present are solid and gaseous conduction and radiation.

Instrumentation

The water-cooled plate is instrumented with nine thin film heat flux gages and ten type K (nickel-chromium/nickel-aluminum) thermocouples. A schematic showing the layout of the thermocouples and heat flux gages on the water-cooled plate is shown in Figure 6. The thermocouple wires are 0.005 inches in diameter (36 gage) and have fiberglass insulation. The thermocouples were installed below the top surface of the water-cooled plate with their junction located typically 0.01 inches below the top surface of the plate. An epoxy filled trench was made on the plate for subsurface burying of thermocouples and thermocouple leads.

Each heat flux gage is one inch long and 0.75 inches wide, with a nominal thickness of 0.006 inches. The gages are thermopiles encapsulated in polyimide film, producing a voltage directly proportional to the impinging heat flux with a nominal sensitivity of 3.3×10^{-6} Volts/[Btu/hr-ft²]. Each heat flux gage also employs a type T (copper/constantan) thermocouple for surface temperature measurement. The heat flux gages were bonded to the top of the water-cooled plate with their lead wires buried underneath the plate top surface. Two epoxy filled trenches were made in the plate for subsurface burying of heat flux gage lead wires. A polyimide sheet 0.005 inches thick covers the plate at locations not covered by heat flux gages. The polyimide sheet was bonded to the plate to provide a uniform surface on the water-cooled plate. The thickness of the bonding agent used for both the heat flux gages and the polyimide sheet was 0.003 inches. The top surface of the polyimide sheet was spray painted using a flat black paint with an emittance value of 0.92 throughout the infrared spectrum.

The septum plate is instrumented with 23 metal sheathed type K thermocouples. The thermocouple leads are 0.0126 inches in diameter (28 gage). The metallic sheath is 304 stainless steel, 0.0625 inches in diameter. The thermocouple junction is formed by welding both leads to the stainless steel sheath. For the installation of thermocouples on the septum plate, small holes 0.01 inches deep and with 45 degree inclination angle with respect to the plate were drilled in the plate at the location of the sensors, and the sheathed thermocouples were inserted into the holes and then welded in place. The thermocouples were installed on the top surface of the septum plate (opposite side from the insulation sample) so that uniform contact between the septum plate and insulation test sample could be maintained. A schematic showing the layout of the thermocouples on the septum plate is shown in Figure 7. The septum plate was oxidized in an oven at 1800°F for 6 hours after the installation of the thermocouples. The emittance of the oxidized Inconel™ has been reported to be 0.8².

The thermocouple and heat flux gage data are collected using a personal-computer-based data acquisition system. The thermocouple data are converted to temperature using look-up tables by the data acquisition software. Raw voltages from the heat flux gages are converted to heat flux by applying a manufacturer-suggested temperature correction to the raw data and then using the manufacturer's linear calibration for heat flux versus voltage for each sensor. The accuracy of the manufacturer's calibration for the range of heat fluxes used in this study was verified by radiant calibration of the heat flux gages using a high intensity irradiance standard (solar constant lamp).

Experimental Procedure

The effective thermal conductivity of different samples are measured with nominal septum plate temperatures of 200, 500, 800, 1100, 1400, 1600, and 1800°F, and nominal environmental pressures of 1×10^{-4} , 1×10^{-3} , 1×10^{-2} , 0.1, 0.5, 1, 5, 10, 100, and 750 torr. The experimental procedure consists of starting the coolant for the water-cooled plate, pumping down the vacuum chamber to approximately 1 torr, and then providing power to the ceramic fiber radiant heater. The power to the heater is controlled using a proportional controller with input from the control thermocouple on the hot plate. The time required to reach the steady-state target temperature varies between 1 to 2 hours. Once the hot plate's temperature is determined to be stable, the chamber is pumped down to 1×10^{-4} torr. Once all the thermocouples and heat flux gages on both the septum and water-cooled plates are stabilized, data storage initiates. Then the vacuum chamber pressure is changed to the next higher value. The tests at each septum plate temperature for the ten different pressures take approximately 90 minutes. During the process of increasing pressure in the vacuum chamber, the chamber is filled with gaseous nitrogen instead of atmospheric air. Filling the chamber with air would introduce water vapor into the chamber, which would significantly increase the time required for pumping-down to low pressures.

Description of test specimen

Four insulation samples were tested, three fibrous insulation samples and one multi-layer insulation. The fibrous insulation samples consisted of Saffil™, Q-Fiber™ felt and Cerachrome™. All the fibrous insulation samples tested were $8 \times 8 \times 0.522$ inches. Saffil™ is made of alumina fibers, Q-Fiber™ felt is made of silica fibers, while Cerachrome™ is composed of silica and alumina fibers. The test matrix included three Saffil™ samples with nominal densities of 1.5, 3, and 6 lb/ft³, two Q-Fiber™ felt samples with nominal densities of 3 and 6 lb/ft³, and two Cerachrome™ samples with nominal densities of 6 and 12 lb/ft³. A listing of the fibrous insulation samples tested in this study is provided in Table 1.

Three different configurations of a multi-layer insulation were tested. The multi-layer insulations, consisting of thin foils coated with high-reflectance coating, were manufactured by S. D. Miller & Associates, Flagstaff, Arizona. The first multi-layer configuration consisted of four foils stacked on top of each other, with a nominal density of 1.5 lb/ft³. The second configuration consisted of nine foils with a nominal density of 3 lb/ft³. No fibrous insulation was used in between the foils for the first two configurations, but a thin layer of Saffil™ with a mass of about six grams was installed between the top of the specimen and the bottom of the septum plate, to prevent accumulation of Inconel™ oxide flakes on the reflective foils. The mass of the Saffil™ was included in the calculation of the effective density. The last configuration consisted of four foils with five Saffil™ spacers, three in between the foils, one on top and one on bottom. The nominal density of this sample was 3 lb/ft³. The three multi-layer configurations employed proprietary design that can not be disclosed in this report. The multi-layer insulation samples were $6 \times 6 \times 0.522$ inches. Since the test set-up is designed for handling 8×8 inch specimen, the multi-layer insulation samples were located in the center of test set-up and a two-inch wide strip of Saffil™ at a nominal density matching that of the corresponding multi-layer insulation was set around the test specimen. A listing of the multi-layer insulation samples tested in this study is provided in Table 2.

Data Analysis

The effective thermal conductivity of the insulation sample is calculated from Fourier's law using the measured heat flux, septum and water-cooled plate temperatures, and sample thickness. Referring to Figure 8, the effective thermal conductivity of the insulation, k , is obtained from:

$$k = \frac{L}{\frac{T_1 - T_3}{q''} - \frac{L'}{k'}} \quad (1)$$

where, T_1 and T_3 are the measured temperatures on top of septum plate and on top of the polyimide sheet bonded to the water-cooled plate, respectively, q'' is the measured heat flux, L and L' are the known insulation and septum plate thicknesses, respectively, and k' is the thermal conductivity of the Inconel™ septum plate assumed to be known.

Only the data from the central five by five inch section of the test set up shown in Figures 6 and 7, referred to as the metered region, are used for calculating the effective thermal conductivity. The effective thermal conductivity of the sample at each of the five heat flux gage locations in the metered region is calculated using Equation (1). Then, the data are averaged to obtain the average effective thermal conductivity. The average cold side temperature is obtained by averaging the measured temperatures on the five heat flux gages in the metered region. The septum plate bottom surface temperatures are calculated from measured temperatures on the septum plate top surface in the metered region, and then averaged to provide the average hot side temperature. The average test specimen temperature is obtained by averaging the average hot and cold side temperatures.

Uncertainty Analysis

An uncertainty analysis was performed to obtain error estimates for the experimentally determined effective thermal conductivity. The procedure for calculating the effective thermal conductivity bias and precision uncertainties is that specified by Coleman and Steele³. The bias error for the estimated effective thermal conductivity, Δk_B , is obtained from:

$$\Delta k_B = \left\{ \left(\frac{\partial k}{\partial L} \Delta L_B \right)^2 + \left(\frac{\partial k}{\partial q''} \Delta q_B'' \right)^2 + \left(\frac{\partial k}{\partial T_2} \Delta T_{2,B} \right)^2 + \left(\frac{\partial k}{\partial T_3} \Delta T_{3,B} \right)^2 \right\}^{\frac{1}{2}} \quad (2)$$

where ΔL_B , $\Delta q_B''$, $\Delta T_{2,B}$, and $\Delta T_{3,B}$ are the bias error estimates for the measurements of insulation thickness, heat flux, septum plate temperature and water-cooled plate temperature, respectively. The precision error for the estimated effective thermal conductivity, Δk_P , is obtained from:

$$\Delta k_P = \left\{ \left(\frac{\partial k}{\partial L} \Delta L_P \right)^2 + \left(\frac{\partial k}{\partial q''} \Delta q_P'' \right)^2 + \left(\frac{\partial k}{\partial T_2} \Delta T_{2,P} \right)^2 + \left(\frac{\partial k}{\partial T_3} \Delta T_{3,P} \right)^2 \right\}^{\frac{1}{2}} \quad (3)$$

where ΔL_P , $\Delta q_P''$, $\Delta T_{2,P}$, and $\Delta T_{3,P}$ are the precision error estimates for the measurements of insulation thickness, heat flux, septum plate temperature and water-cooled plate temperature, respectively. The overall uncertainty in the estimation of the effective thermal conductivity, Δk_U , is obtained by combining the precision and bias error using the root-sum-square method⁴:

$$\Delta k_U = \left\{ (\Delta k_B)^2 + (\Delta k_P)^2 \right\}^{\frac{1}{2}} \quad (4)$$

The bias error for the thermocouples was determined by performing a comparison calibration in a controlled-temperature oven/bath with a NIST-traceable thermometer. The bias error for heat flux sensors was determined by calibration against a high intensity irradiance standard (solar constant lamp). The precision error for the thermocouples and heat flux gages was determined from the experimental measurements, by calculating the standard deviations of the temporal variations of each measured quantity. The bias and precision error estimates for measurements of the insulation thickness, heat flux, septum plate and water-cooled plate temperatures are tabulated in Table 3. The bias, precision, and overall uncertainties for effective thermal conductivity are presented in Table 4. The uncertainties are presented as a percentage of uncertainty with respect to the calculated thermal conductivity. Data presented in the table are from measurements on Saffil™ at 1.5 lb/ft³, and correspond to measurements at pressures of 1×10⁻⁴, 1×10⁻², and 760 torr, and nominal sample average temperatures of 125, 580, and 950°F. The overall uncertainty varied between 5.5 to 9.7 percent.

To provide an independent assessment of the uncertainty of the effective thermal conductivity measurements, the effective thermal conductivity of fumed silica board, Standard Reference Material (SRM)1459 from the National Institute of Standard and Technology (NIST) was measured. The silica board was 12 × 12 × 1 inches, and its reported thermal conductivity at one atmosphere and at 75.°F is 0.012 Btu/(hr ft °F). The effective thermal conductivity of the SRM sample was measured by Holometrix, Inc using the ASTM standard C-177⁴ entitled “Standard Test Method for Steady-State Heat Flux Measurements and Thermal Transmission Properties by Means of the Guarded-Hot-Plate Apparatus,” at mean temperatures up to 571°F, and the results are tabulated in Tabulated in Table 5. The results of the measurements using the present apparatus are provided in Table 6. The average specimen temperature, the measured effective thermal conductivity using the present apparatus, and the corresponding thermal conductivity measurement from the guarded hot plate data obtained from interpolating data in Table 5 are presented. The percentage error between measurements using the current apparatus and the guarded hot plate data are also presented. The data from the current apparatus are to within ±5.5% of guarded hot plate data. It should be noted that the measurements were performed with a cold side temperature of approximately 85°F, with hot side temperatures of 128.1, 129.1, and 203.7°F. Thus, the temperature gradient through the specimen was significantly higher compared to the guarded hot plate technique. Furthermore, the present apparatus is not intended for making measurements on solid specimen, since it doesn’t have any provisions for applying compressive forces on the sample to ensure good thermal contact between the sample and the hot and cold plates. The present apparatus was designed for measurements on fibrous insulation, where most of the heat transfer is through gas conduction and radiation and perfect thermal contact is not required. Despite this difference in measurement techniques, the difference in measured values using the two techniques was within the uncertainty limits presented in Table 4.

Results and Discussion

The experimental effective thermal conductivities of Saffil™ at nominal densities of 1.5, 3, and 6 lb/ft³ are tabulated in Tables 7, 8, and 9, respectively. The entries in each table include the environmental pressure in the chamber, average cold side temperature, average hot side temperature, average specimen temperature obtained by averaging the average hot and cold side temperatures, the calculated effective thermal conductivity, and the product of density and thermal conductivity. Temperature in the tables are in degrees Fahrenheit, the thermal conductivity is given in units of $\frac{Btu-in}{hr-F-ft^2}$, while the product of density and thermal conductivity is given in units of $\frac{Btu-in}{hr-F-ft^2} \frac{lb}{ft^3}$. The experimental effective thermal

conductivities of Q-Fiber™ at nominal densities of 3 and 6 lb/ft³ are tabulated in Tables 10 and 11, respectively. Data for the measurements on Cerachrome™ at nominal densities of 6 and 12 lb/ft³ are presented in Tables 12 and 13, respectively. Data on the three multi-layer configurations are presented in Tables 14, 15, and 16.

The effective thermal conductivity of various samples as a function of average temperature for environmental pressures of 1×10^{-3} , 1×10^{-1} , 1, 10, and 100 torr are shown in Figures 9a through 9e, respectively. The effective thermal conductivity varies non-linearly with sample average temperature, increasing rapidly with increasing temperature due to the nonlinear nature of radiation heat transfer. This effect is more evident with lower density insulations. As the insulation density increases the solid conduction contribution to the overall heat transfer increases, but the radiation heat transfer decreases more rapidly, resulting in a net decrease in the effective thermal conductivity. At lower pressures, the multi-layer insulations have the lowest thermal conductivity. At higher pressures (above 10 torr), Saffil™ and Q-Fiber™ at 6 lb/ft³ provide the lowest thermal conductivity. Cerachrome™ at 6 lb/ft³ and Saffil™ at 1.5 lb/ft³ provided the highest effective thermal conductivities at all pressures.

Since the effective thermal conductivities of samples were obtained at different sample densities, the product of thermal conductivity and density provides a good comparative quantity for comparing the steady-state effectiveness of various samples. For steady-state heat transfer the product of thermal conductivity and density can be shown to be proportional to the mass of insulation required per unit area. The lightest weight insulation will have the lowest value of the product of thermal conductivity and density for steady-state heat transfer. The same trend may hold for slowly varying transient situations. The product of effective thermal conductivity and density of various samples as a function of sample average temperature for environmental pressures of 1×10^{-3} , 1×10^{-1} , 1, 10, and 100 torr are shown in Figures 10a through 10e, respectively. In Figure 10a the Cerachrome™ samples at 6 and 12 lb/ft³ provided the highest thermal conductivity density product at environmental pressure of 1×10^{-3} torr, 2 to 3 times higher than all the other samples. The same trend continued for all the other environmental pressures tested. Therefore, data from Cerachrome™ were deleted for Figures 10b through 10e to enable better comparison of data from other samples. The three multi-layer insulation configurations provided the best performance over the entire pressure and temperature range. The performance of Saffil™ and Q-Fiber™ felt were similar under all measured conditions.

At low pressures, where gas conduction is negligible, all densities of Saffil™ and Q-Fiber™ had nearly the same thermal conductivity density product at a given temperature. This implies that in the absence of gas conduction, the mass of insulation required may be insensitive to the density of the insulation.

The effective thermal conductivity of various samples as a function of environmental pressure for nominal sample average temperatures of 125, 275, 425, 730, and 950°F are shown in Figures 11a through 11e, respectively. As can be seen, gas conduction is negligible up to 0.1 torr, rapidly increases between 0.1 and 10 torr, and then stays relatively constant between 100 and 760 torr.

Concluding Remarks

A simple experimental apparatus was designed to measure the effective thermal conductivity of various high temperature insulations subject to large temperature gradients representative of typical launch vehicle re-entry conditions. The insulation sample cold side could be maintained around room temperature, while the hot side could be heated to temperatures as high as 1800°F. The environmental pressure could be varied from 1×10^{-4} to 760 torr. The results of an uncertainty analysis yielded an

overall uncertainty of 5.5 to 9.9 percent for the effective thermal conductivity measurements. Thermal conductivity measurements on a fumed silica reference material from NIST at atmospheric pressure were within 5.5 percent of reported data.

Effective thermal conductivities were measured for the following insulation samples: Saffil™ at 1.5, 3, 6 lb/ft³, Q-Fiber™ felt at 3, 6 lb/ft³, Cerachrome™ at 6, 12 lb/ft³, and three multi-layer insulation configurations at 1.5 and 3 lb/ft³. Comparison of data showed that Cerachrome™ was a much less effective insulator than the other insulations tested, and that Saffil™ and Q-Fiber™ felt were comparable in performance under all tested conditions. The three multi-layer configurations provided best performance over the entire pressure and temperature range.

References

1. ASTM Standard C 201: "Standard Test Method for Thermal Conductivity of Refractories," 1996 Annual Book of ASTM Standards, Vol. 15.01, *Refractories, Carbon and Graphite Products, Activated Carbon Advanced Ceramics*, 1996.
2. Clark, R.K., Unnam, J., "Response of Inconel 617 to Sea Salt and Re-entry Conditions," *Journal of Spacecraft*, Vol. 23, No. 1, Jan-Feb 1986, pp. 96- 101
3. Coleman, H.W., Steele, W.G., *Experimentation and Uncertainty Analysis for Engineers*, 1989, John Wiley & Sons, Inc.
4. ASTM Standard C 177: "Standard Test Method for Steady-State Heat Flux Measurements and Thermal Transmission Properties by Means of the Guarded-Hot-Plate Apparatus," 1996 Annual Book of ASTM Standards, Vol. 4.06, *Thermal Insulation, Environmental Acoustics*, 1996.

Table 1. Description of fibrous insulation test specimen. Specimen were $8 \times 8 \times 0.522$ inches

Specimen	Nominal density (lb/ft ³)	Actual density (lb/ft ³)
Saffil™	1.5	1.52
Saffil™	3	3.03
Saffil™	6	6.0
Q-Fiber™ felt	3	3.03
Q-Fiber™ felt	6	5.97
Cerachrome™	6	5.93
Cerachrome™	12	12.0

Table 2. Description of multi-layer insulation test specimen. Specimen were $6 \times 6 \times 0.522$ inches

Specimen	Description	Mass of foils (grams)	Mass of Saffil™ (grams)	Nominal density (lb/ft ³)	Actual density (lb/ft ³)
Multi-layer configuration 1	4 foils	7.74	0.53*	1.5	1.49
Multi-layer configuration 2	9 foils	14.04	0.7*	3	3
Multi-layer configuration 3	4 foils with five Saffil spacers	5.59	9.08	3	2.97

* indicates mass of Saffil™ layer sandwiched between the top of specimen and bottom of septum plate

Table 3. Bias and precision uncertainties for experimentally measured quantities

Measurement	Bias error	Precision error
insulation thickness (in)	0.01	0.02
heat flux (Btu/hr-ft ²)	3.4% of reading	1.14 – 8.5
Septum plate temperature (°F)	6.4	0.29 – 0.76
Water-cooled plate temperature (°F)	0.18	0.36 - .4

Table 4. Overall uncertainty estimates for effective thermal conductivity. Estimates obtained from data on Saffil™ at 1.5 lb/ft³

Pressure (torr)	Average Temperature (°F)	Bias Error (%)	Precision Error (%)	Overall Error (%)
0.0001	124.8	5.86	7.68	9.66
0.01	124.7	5.86	7.29	9.35
760	123.9	5.96	4.73	7.61
0.0001	577.9	3.98	3.87	5.55
0.0105	578.1	3.98	3.87	5.55
755	577.1	3.97	3.85	5.53
0.0001	941.1	3.91	3.82	5.47
0.0114	941.3	3.91	3.84	5.48
474	943.1	3.91	3.82	5.47

Table 5. Effective thermal conductivity of NIST Standard Reference Material 1459 measured using the guarded hot plate technique

Average Temperature (°F)	Effective thermal conductivity (Btu/ft-hr-°F)
73	0.0121
210	.0129
391	.0139
571	.0165

Table 6. Comparison of effective thermal conductivity measurements on NIST Standard Reference Material 1459 using the present apparatus and the guarded hot plate technique

Average Temperature (°F)	Thermal conductivity, present apparatus (Btu/ft-hr-°F)	Thermal Conductivity, guarded hot plate technique (Btu/ft-hr-°F)	Percent difference (%)
128.1	.0129	.0124	2.3
129.1	.0129	.0124	2.3
203.7	.0122	.0129	5.5

Table 7. Effective thermal conductivity of Saffil™ at nominal density of 1.5 lb/ft³

P (torr)	T_cold °F	T_hot °F	T_avg °F	k Btu-in hr-ft ² -°F	ρk Btu-in-lb hr-ft ⁵ -°F	P (torr)	T_cold °F	T_hot °F	T_avg °F	k Btu-in hr-ft ² -°F	ρk Btu-in-lb hr-ft ⁵ -°F
1 x10 ⁻⁴	50.7	198.9	124.8	0.0606	0.0920	1.4x10 ⁻⁴	67.9	1394.8	731.4	0.5086	0.7730
1x10 ⁻³	50.7	200.0	125.3	0.0612	0.0930	1.06x10 ⁻³	67.9	1394.9	731.4	0.5092	0.7740
1x10 ⁻²	50.6	198.8	124.7	0.0686	0.1042	1x10 ⁻²	68.1	1394.8	731.4	0.5157	0.7838
0.1	50.9	199.3	125.1	0.1074	0.1632	0.1	69.5	1394.2	731.8	0.5515	0.8383
1	51.6	197.7	124.6	0.2121	0.3224	1.025	74.2	1391.9	733.0	0.7055	1.0723
10	51.9	197.5	124.7	0.2716	0.4128	10.1	79.9	1388.0	734.0	0.8999	1.3678
100	52.2	196.7	124.4	0.2818	0.4284	100	81.6	1385.2	733.4	0.9408	1.4300
760	52.2	195.6	123.9	0.2846	0.4326	754	81.7	1383.0	732.3	0.9350	1.4212
1 x10 ⁻⁴	53.4	501.5	277.5	0.1164	0.1769	1.01x10 ⁻⁴	78.8	1592.4	835.6	0.6658	1.0120
1x10 ⁻³	53.3	501.4	277.4	0.1169	0.1778	1.045x10 ⁻³	78.7	1592.7	835.7	0.6658	1.0120
1.05x10 ⁻²	53.3	501.3	277.3	0.1242	0.1888	1.045x10 ⁻²	79.0	1592.8	835.9	0.6709	1.0198
0.1	53.8	500.8	277.3	0.1613	0.2452	0.1005	80.6	1592.6	836.6	0.7045	1.0709
1	55.2	499.1	277.1	0.2854	0.4338	1	86.2	1590.6	838.4	0.8581	1.3043
10	56.1	497.5	276.8	0.3766	0.5725	10.25	94.2	1586.8	840.5	1.0810	1.6431
100	56.3	496.2	276.3	0.3908	0.5940	100.15	96.8	1583.6	840.2	1.1336	1.7231
760	56.6	493.9	275.3	0.3938	0.5985	755	96.4	1581.3	838.9	1.1264	1.7121
1 x10 ⁻⁴	54.5	796.8	425.6	0.2049	0.3115	1 x10 ⁻⁴	90.3	1791.8	941.1	0.8504	1.2926
1x10 ⁻³	54.4	797.0	425.7	0.2060	0.3131	1.048x10 ⁻³	90.4	1791.9	941.1	0.8501	1.2921
1.01x10 ⁻²	54.4	797.0	425.7	0.2128	0.3235	1.14x10 ⁻²	90.7	1792.0	941.3	0.8546	1.2991
0.1	55.2	796.3	425.7	0.2495	0.3793	0.1994	92.6	1791.3	942.0	0.8927	1.3569
1	57.6	794.7	426.1	0.3852	0.5854	1.019	99.1	1788.9	944.0	1.0578	1.6078
10	59.7	792.4	426.0	0.5101	0.7754	10.25	108.6	1784.4	946.5	1.2956	1.9693
100	59.9	790.3	425.1	0.5308	0.8068	99.9	111.4	1779.0	945.2	1.3542	2.0584
760	59.9	787.4	423.6	0.5311	0.8073	474	110.6	1775.7	943.1	1.3410	2.0383
1 x10 ⁻⁴	59.4	1096.4	577.9	0.3281	0.4987						
1x10 ⁻³	59.7	1096.5	578.1	0.3291	0.5002						
1.05x10 ⁻²	59.8	1096.4	578.1	0.3356	0.5102						
0.104	60.9	1095.8	578.4	0.3715	0.5647						
1	64.6	1093.5	579.1	0.5142	0.7816						
10.4	67.9	1090.1	579.0	0.6744	1.0251						
100.4	69.1	1087.3	578.2	0.7046	1.0710						
755	69.1	1085.1	577.1	0.7021	1.0673						

Table 8. Effective thermal conductivity of Saffil™ at nominal density of 3 lb/ft³

P (torr)	T_cold °F	T_hot °F	T_avg °F	k Btu-in hr-ft ² -°F	ρk Btu-in-lb hr-ft ⁵ -°F	P (torr)	T_cold °F	T_hot °F	T_avg °F	k Btu-in hr-ft ² -°F	ρk Btu-in-lb hr-ft ⁵ -°F
1 x10 ⁻⁴	49.4	200.9	125.2	0.0356	0.0905	1 x10 ⁻⁴	62.1	1392.9	727.5	0.2727	0.0905
1x10 ⁻³	49.6	201.3	125.4	0.0366	0.0905	1.09x10 ⁻³	62.2	1393.0	727.6	0.2733	0.0905
1.03x10 ⁻²	49.7	201.4	125.5	0.0430	0.0905	1.09x10 ⁻²	62.4	1392.9	727.7	0.2770	0.0905
0.0997	49.9	201.1	125.5	0.0667	0.0905	0.1	63.6	1392.5	728.0	0.2966	0.0905
1	50.5	199.8	125.2	0.1535	0.0905	0.5035	66.0	1391.3	728.6	0.3547	0.0905
10.1	51.0	199.4	125.2	0.2213	0.0905	1	67.2	1390.4	728.8	0.4002	0.0905
99.8	51.5	198.5	125.0	0.2375	0.0905	5	71.0	1388.1	729.6	0.5257	0.0905
745	52.0	197.4	124.7	0.2422	0.0905	10.2	72.3	1386.8	729.6	0.5647	0.0905
1.01 x10 ⁻⁴	52.4	505.1	278.8	0.0644	0.0905	99.9	74.7	1384.5	729.6	0.6231	0.0905
1.004x10 ⁻³	52.5	505.1	278.8	0.0653	0.0905	749	75.2	1382.1	728.7	0.6363	0.0905
1.05x10 ⁻²	52.5	505.2	278.8	0.0700	0.0905	1 x10 ⁻⁴	68.6	1592.4	830.5	0.3518	0.0905
0.101	52.7	504.9	278.8	0.0927	0.0905	1.01x10 ⁻³	68.8	1592.5	830.7	0.3524	0.0905
0.999	54.1	497.7	275.9	0.1888	0.0905	1.04x10 ⁻²	69.2	1592.5	830.8	0.3555	0.0905
10.4	54.2	495.6	274.9	0.2813	0.0905	0.102	70.5	1592.1	831.3	0.3750	0.0905
99.8	54.4	494.1	274.3	0.3049	0.0905	0.499	72.8	1591.0	831.9	0.4316	0.0905
750	54.4	492.3	273.3	0.3115	0.0905	0.996	74.3	1590.2	832.2	0.4778	0.0905
1. 01x10 ⁻⁴	53.4	794.5	423.9	0.1129	0.0905	4.98	78.6	1587.9	833.3	0.6117	0.0905
1.07x10 ⁻³	53.3	794.6	424.0	0.1137	0.0905	10.3	79.8	1586.5	833.2	0.6585	0.0905
1.12x10 ⁻²	53.6	794.6	424.1	0.1179	0.0905	99.9	82.7	1583.8	833.2	0.7264	0.0905
0.103	54.2	794.1	424.2	0.1402	0.0905	750	83.3	1581.7	832.5	0.7407	0.0905
0.302	55.1	793.5	424.3	0.1727	0.0905	1. 5x10 ⁻⁴	77.6	1790.7	934.2	0.4473	0.0905
1	56.2	792.4	424.3	0.2395	0.0905	1.15x10 ⁻³	77.6	1790.8	934.2	0.4477	0.0905
4.99	58.0	790.2	424.1	0.3324	0.0905	1.05x10 ⁻²	77.0	1790.7	933.8	0.4509	0.0905
10.3	58.5	789.4	424.0	0.3568	0.0905	0.107	78.5	1790.2	934.4	0.4703	0.0905
99.9	58.9	787.4	423.1	0.3897	0.0905	0.504	81.6	1789.1	935.4	0.5275	0.0905
750	59.2	785.2	422.2	0.3982	0.0905	0.9985	83.5	1788.2	935.8	0.5752	0.0905
1x10 ⁻⁴	60.9	1095.4	578.2	0.1811	0.0905	4.99	87.6	1785.2	936.4	0.7570	0.0905
1.03x10 ⁻³	60.7	1095.5	578.1	0.1815	0.0905	10.5	89.1	1783.6	936.3	0.8034	0.0905
1.09x10 ⁻²	60.0	1095.5	577.8	0.1852	0.0905	99.85	92.2	1779.9	936.0	0.8675	0.0905
0.1	59.6	1095.2	577.4	0.2055	0.0905	296	92.4	1777.8	935.1	0.8393	0.0905
0.5	62.2	1094.1	578.2	0.2643	0.0905						
1	63.6	1093.3	578.5	0.3081	0.0905						
5	66.4	1091.1	578.8	0.4186	0.0905						
10.3	66.0	1089.8	577.9	0.4500	0.0905						
99.9	67.1	1087.7	577.4	0.4946	0.0905						
750	66.6	1085.7	576.2	0.5052	0.0905						

Table 9. Effective thermal conductivity of Saffil™ at nominal density of 6 lb/ft³

P (torr)	T_cold °F	T_hot °F	T_avg °F	k Btu-in hr-ft ² -°F	ρk Btu-in-lb hr-ft ⁵ -°F	P (torr)	T_cold °F	T_hot °F	T_avg °F	k Btu-in hr-ft ² -°F	ρk Btu-in-lb hr-ft ⁵ -°F
1.08 x10 ⁻⁴	55.2	201.7	128.4	0.0223	0.1337	.997x10 ⁻⁴	62.9	1394.4	728.6	0.1380	0.8282
0.998x10 ⁻³	55.2	201.6	128.4	0.0227	0.1363	1.01x10 ⁻³	63.0	1394.7	728.9	0.1387	0.8320
0.99x10 ⁻²	55.4	201.9	128.6	0.0251	0.1505	1.04x10 ⁻²	63.6	1394.7	729.1	0.1407	0.8442
0.101	55.7	201.7	128.7	0.0416	0.2498	0.102	64.6	1394.4	729.5	0.1511	0.9067
0.501	56.1	201.2	128.6	0.0806	0.4837	0.509	66.0	1393.4	729.7	0.1807	1.0840
1	56.3	200.4	128.4	0.1049	0.6295	0.999	66.0	1392.4	729.2	0.2077	1.2463
4.99	56.7	199.6	128.1	0.1660	0.9958	4.995	69.9	1390.0	729.9	0.3153	1.8916
10.2	56.8	199.4	128.1	0.1828	1.0969	10.4	71.7	1388.3	730.0	0.3611	2.1664
99.4	56.9	199.2	128.1	0.2078	1.2470	98.95	75.0	1385.2	730.1	0.4405	2.6429
751	57.0	198.0	127.5	0.2152	1.2915	750	75.7	1383.0	729.3	0.4625	2.7751
1 x10 ⁻⁴	55.4	499.6	277.5	0.0362	0.2174	1.05 x10 ⁻⁴	65.2	1596.4	830.8	0.1756	1.0539
1.02x10 ⁻³	55.4	499.6	277.5	0.0372	0.2229	1.08x10 ⁻³	65.3	1596.5	830.9	0.1765	1.0588
1.02x10 ⁻²	55.5	499.7	277.6	0.0400	0.2401	1.05x10 ⁻²	65.7	1596.6	831.1	0.1788	1.0727
0.1	55.7	499.7	277.7	0.0538	0.3228	0.107	66.7	1596.0	831.4	0.1885	1.1311
0.498	56.3	498.5	277.4	0.0865	0.5191	0.502	68.6	1595.4	832.0	0.2168	1.3009
1	56.8	498.2	277.5	0.1151	0.6907	1	69.7	1594.6	832.2	0.2441	1.4647
4.99	57.7	496.5	277.1	0.1924	1.1545	5.01	74.5	1592.1	833.3	0.3554	2.1326
10.5	58.1	495.9	277.0	0.2160	1.2960	10.4	76.4	1590.7	833.5	0.4061	2.4366
99.9	58.5	494.6	276.5	0.2507	1.5042	99.85	80.9	1587.9	834.4	0.4966	2.9798
748	58.5	492.5	275.5	0.2615	1.5690	1 x10 ⁻⁴	69.8	1795.6	932.7	0.2216	1.3297
.998x10 ⁻⁴	56.3	794.9	425.6	0.0592	0.3550	1.07x10 ⁻³	69.9	1795.9	932.9	0.2225	1.3349
1.12x10 ⁻³	56.3	794.8	425.5	0.0602	0.3610	1.09x10 ⁻²	70.4	1796.1	933.2	0.2247	1.3481
1.1x10 ⁻²	56.3	794.9	425.6	0.0631	0.3787	0.09985	71.5	1795.8	933.6	0.2339	1.4033
0.102	57.0	794.8	425.9	0.0752	0.4514	0.5005	73.5	1794.9	934.2	0.2620	1.5722
0.507	58.1	793.8	425.9	0.1088	0.6531	1.02	74.9	1794.2	934.5	0.2903	1.7420
1	58.7	792.9	425.8	0.1357	0.8142	4.99	80.2	1791.9	936.0	0.4051	2.4307
4.99	60.7	790.6	425.6	0.2254	1.3525	10.5	83.3	1790.2	936.7	0.4615	2.7687
10.5	61.4	789.9	425.6	0.2567	1.5403	100	88.5	1786.9	937.7	0.5639	3.3835
100	62.7	787.5	425.1	0.3044	1.8267	749	89.9	1785.1	937.5	0.5945	3.5672
750	63.1	785.7	424.4	0.3185	1.9109						
1.02 x10 ⁻⁴	58.5	1094.6	576.5	0.0925	0.5552						
1.01x10 ⁻³	58.7	1094.7	576.7	0.0934	0.5604						
1.04x10 ⁻²	59.0	1094.9	576.9	0.0955	0.5730						
0.104	59.8	1094.6	577.2	0.1062	0.6372						
0.5	61.0	1093.7	577.4	0.1380	0.8277						
1	61.9	1092.8	577.3	0.1660	0.9959						
5.02	64.8	1090.4	577.6	0.2663	1.5975						
10.5	65.8	1089.0	577.4	0.3051	1.8305						
99	67.8	1086.6	577.2	0.3673	2.2040						
747	68.2	1084.9	576.5	0.3847	2.3081						

Table 10. Effective thermal conductivity of Q-Fiber™ felt at nominal density of 3 lb/ft³

P (torr)	T_cold °F	T_hot °F	T_avg °F	k Btu-in hr-ft ² -°F	ρk Btu-in-lb hr-ft ⁵ -°F	P (torr)	T_cold °F	T_hot °F	T_avg °F	k Btu-in hr-ft ² -°F	ρk Btu-in-lb hr-ft ⁵ -°F
1 x10 ⁻⁴	56.3	199.1	127.7	0.0456	0.1382	1 x10 ⁻⁴	67.7	1392.4	730.1	0.3010	0.9120
1.02x10 ⁻³	56.3	199.1	127.7	0.0468	0.1419	1x10 ⁻³	67.7	1392.5	730.1	0.3014	0.9133
1.005x10 ⁻²	56.2	199.2	127.7	0.0495	0.1501	1.03x10 ⁻²	67.8	1392.7	730.3	0.3037	0.9204
0.109	56.3	199.2	127.8	0.0662	0.2007	0.103	68.5	1392.5	730.5	0.3162	0.9580
0.499	56.6	199.3	128.0	0.1032	0.3128	0.508	69.9	1392.0	730.9	0.3497	1.0595
0.997	56.9	199.0	127.9	0.1297	0.3931	1	70.9	1391.4	731.2	0.3791	1.1487
4.99	57.2	198.4	127.8	0.1985	0.6014	5	74.8	1389.8	732.3	0.4962	1.5036
10.8	57.3	198.2	127.7	0.2192	0.6643	10	76.4	1388.9	732.7	0.5516	1.6713
99.4	57.4	197.3	127.4	0.2465	0.7470	100	80.2	1387.4	733.8	0.6470	1.9605
750	57.4	195.6	126.5	0.2544	0.7708	760	81.1	1385.5	733.3	0.6648	2.0144
1 x10 ⁻⁴	57.3	496.8	277.1	0.0792	0.2400	1.02 x10 ⁻⁴	72.7	1595.1	833.9	0.3765	1.1408
1x10 ⁻³	57.3	497.0	277.2	0.0796	0.2413	1.08x10 ⁻³	72.7	1595.2	834.0	0.3769	1.1419
1.01x10 ⁻²	57.4	497.2	277.3	0.0827	0.2506	1.02x10 ⁻²	72.9	1595.1	834.0	0.3789	1.1481
0.1	57.8	497.3	277.5	0.0968	0.2933	0.10015	73.7	1595.0	834.4	0.3910	1.1847
0.499	58.2	497.0	277.6	0.1330	0.4029	0.5015	75.4	1594.4	834.9	0.4240	1.2849
1	58.7	496.8	277.7	0.1620	0.4909	1	76.7	1593.8	835.3	0.4537	1.3748
4.98	59.7	495.8	277.8	0.2470	0.7483	4.99	81.3	1592.0	836.6	0.5752	1.7430
10.8	60.2	495.4	277.8	0.2770	0.8393	10.5	83.6	1590.8	837.2	0.6349	1.9236
99.6	60.8	495.0	277.9	0.3180	0.9634	100.3	88.5	1588.0	838.2	0.7448	2.2568
750	61.0	493.2	277.1	0.3273	0.9916	748	89.3	1586.0	837.7	0.7654	2.3191
1 x10 ⁻⁴	59.7	792.0	425.8	0.1345	0.4076	1 x10 ⁻⁴	78.9	1792.9	935.9	0.4609	1.3964
1x10 ⁻³	59.6	792.3	425.9	0.1351	0.4093	1x10 ⁻³	78.9	1793.0	935.9	0.4612	1.3973
1x10 ⁻²	59.8	792.6	426.2	0.1374	0.4162	1.02x10 ⁻²	79.1	1792.9	936.0	0.4633	1.4038
0.1005	59.9	792.8	426.4	0.1503	0.4555	0.103	80.2	1792.8	936.5	0.4758	1.4416
0.5	60.6	793.1	426.9	0.1862	0.5643	0.51	82.3	1792.3	937.3	0.5091	1.5426
1	61.5	792.9	427.2	0.2162	0.6550	1	83.8	1791.7	937.7	0.5383	1.6312
5.02	63.6	792.3	427.9	0.3152	0.9550	4.99	89.4	1789.3	939.3	0.6639	2.0117
10.8	64.4	791.8	428.1	0.3539	1.0722	10.5	91.8	1787.9	939.8	0.7283	2.2069
99.6	65.7	791.1	428.4	0.4108	1.2446	100	97.0	1784.7	940.8	0.8523	2.5825
748	65.8	789.1	427.5	0.4221	1.2789	749	98.7	1781.7	940.2	0.8753	2.6522
1 x10 ⁻⁴	62.8	1095.0	578.9	0.2085	0.6317						
1x10 ⁻³	62.9	1095.1	579.0	0.2089	0.6331						
1x10 ⁻²	63.0	1095.2	579.1	0.2116	0.6412						
0.101	63.7	1095.1	579.4	0.2238	0.6782						
0.517	64.9	1094.6	579.7	0.2592	0.7855						
1	65.7	1094.1	579.9	0.2882	0.8733						
5	68.5	1093.1	580.8	0.3974	1.2043						
10.65	70.0	1091.9	580.9	0.4444	1.3466						
99.7	72.2	1090.7	581.5	0.5204	1.5769						
748	72.9	1088.4	580.6	0.5342	1.6186						

Table 11. Effective thermal conductivity of Q-Fiber™ felt at nominal density of 6 lb/ft³

P (torr)	T_cold °F	T_hot °F	T_avg °F	k Btu-in hr-ft ² -°F	ρk Btu-in-lb hr-ft ⁵ -°F	P (torr)	T_cold °F	T_hot °F	T_avg °F	k Btu-in hr-ft ² -°F	ρk Btu-in-lb hr-ft ⁵ -°F
1.03 x10 ⁻⁴	56.1	199.8	127.9	0.0346	0.2063	1.01 x10 ⁻⁴	61.2	1393.6	727.4	0.1646	0.9829
1.03x10 ⁻³	55.9	200.0	128.0	0.0348	0.2079	1.06x10 ⁻³	61.2	1393.7	727.4	0.1652	0.9861
1.02x10 ⁻²	56.0	199.7	127.8	0.0380	0.2271	1.015x10 ⁻²	61.4	1393.8	727.6	0.1668	0.9959
0.102	56.2	199.5	127.9	0.0506	0.3021	0.1025	62.0	1393.7	727.8	0.1735	1.0355
0.503	56.4	199.4	127.9	0.0758	0.4526	0.51	63.2	1393.2	728.2	0.1932	1.1534
1	56.6	199.3	128.0	0.0946	0.5648	1	64.0	1392.7	728.3	0.2106	1.2574
4.99	56.8	198.6	127.7	0.1585	0.9462	4.99	66.9	1391.1	729.0	0.2940	1.7554
10.3	57.0	197.9	127.4	0.1836	1.0962	10.5	68.4	1390.0	729.2	0.3434	2.0502
99.3	57.2	196.8	127.0	0.2255	1.3460	100	72.2	1388.0	730.1	0.4571	2.7288
748	57.0	194.4	125.7	0.2375	1.4178	748	73.5	1385.8	729.7	0.4909	2.9308
1.02 x10 ⁻⁴	54.8	497.4	276.1	0.0500	0.2983	1.02 x10 ⁻⁴	63.9	1593.3	828.6	0.2022	1.2069
1.015x10 ⁻³	54.9	497.7	276.3	0.0515	0.3072	1x10 ⁻³	63.9	1593.4	828.7	0.2028	1.2105
1.01x10 ⁻²	54.9	497.7	276.3	0.0531	0.3168	1.01x10 ⁻²	64.0	1593.4	828.7	0.2044	1.2202
0.102	55.2	497.5	276.3	0.0626	0.3736	0.1015	64.8	1593.2	829.0	0.2109	1.2591
0.501	55.5	496.6	276.1	0.0845	0.5047	0.505	66.0	1592.6	829.3	0.2294	1.3696
1	55.7	496.0	275.9	0.1040	0.6207	0.999	66.7	1592.1	829.4	0.2467	1.4726
4.99	56.6	494.5	275.6	0.1774	1.0591	4.99	70.1	1590.0	830.1	0.3309	1.9756
10.3	56.9	493.8	275.4	0.2092	1.2492	10.5	72.0	1588.9	830.5	0.3837	2.2908
100.4	57.7	492.6	275.2	0.2661	1.5884	99.8	76.9	1586.2	831.5	0.5105	3.0475
745	58.0	491.2	274.6	0.2833	1.6911	748	78.5	1584.0	831.2	0.5488	3.2765
1 x10 ⁻⁴	56.4	795.7	426.0	0.0773	0.4615	1.03 x10 ⁻⁴	67.6	1791.8	929.7	0.2454	1.4652
1.03x10 ⁻³	56.7	796.1	426.4	0.0797	0.4758	0.965x10 ⁻³	67.6	1792.0	929.8	0.2459	1.4682
1.03x10 ⁻²	56.8	796.2	426.5	0.0817	0.4878	1.02x10 ⁻²	67.7	1792.2	929.9	0.2476	1.4781
0.1045	57.1	796.1	426.6	0.0906	0.5409	0.103	68.5	1792.2	930.4	0.2540	1.5164
0.504	57.6	795.4	426.5	0.1120	0.6689	0.501	69.9	1791.8	930.8	0.2723	1.6257
0.994	58.0	794.9	426.4	0.1303	0.7778	1	70.8	1791.3	931.0	0.2894	1.7278
5.005	59.6	793.2	426.4	0.2087	1.2462	5.01	74.8	1789.5	932.1	0.3755	2.2415
10.4	60.2	792.2	426.2	0.2471	1.4750	10.4	77.1	1788.0	932.5	0.4302	2.5684
99.9	61.7	790.9	426.3	0.3220	1.9221	100.3	83.1	1784.5	933.8	0.5718	3.4134
746	62.1	789.0	425.6	0.3441	2.0544	748	85.0	1782.2	933.6	0.6143	3.6672
1.01 x10 ⁻⁴	58.1	1095.3	576.7	0.1159	0.6919						
1.025x10 ⁻³	58.0	1095.7	576.8	0.1173	0.7003						
1.025x10 ⁻²	58.0	1095.8	576.9	0.1193	0.7123						
0.101	58.1	1095.7	576.9	0.1269	0.7578						
0.499	59.2	1095.3	577.2	0.1473	0.8794						
1	59.9	1094.7	577.3	0.1652	0.9863						
5.025	62.2	1093.3	577.8	0.2478	1.4794						
10.6	63.3	1092.2	577.8	0.2920	1.7432						
100.1	66.0	1090.1	578.0	0.3861	2.3050						
748	66.5	1088.4	577.5	0.4133	2.4671						

Table 12. Effective thermal conductivity of Cerachrome™ at nominal density of 6 lb/ft³

P (torr)	T_cold °F	T_hot °F	T_avg °F	k Btu-in hr-ft ² -°F	ρk Btu-in-lb hr-ft ⁵ -°F	P (torr)	T_cold °F	T_hot °F	T_avg °F	k Btu-in hr-ft ² -°F	ρk Btu-in-lb hr-ft ⁵ -°F
1 x10 ⁻⁴	51.0	199.1	125.1	0.0708	0.4200	1.03 x10 ⁻⁴	68.6	1391.0	729.8	0.6402	3.7965
1x10 ⁻³	51.2	199.7	125.5	0.0721	0.4276	.997x10 ⁻³	68.8	1391.1	729.9	0.6413	3.8030
1.025x10 ⁻²	51.5	200.0	125.8	0.0820	0.4863	1.06x10 ⁻²	69.3	1391.0	730.1	0.6489	3.8479
0.103	52.0	199.7	125.8	0.1259	0.7467	0.1015	70.6	1390.5	730.6	0.6844	4.0588
0.499	52.4	198.3	125.3	0.1998	1.1846	0.503	73.3	1389.3	731.3	0.7717	4.5759
1	52.4	197.9	125.1	0.2359	1.3986	1	75.2	1388.3	731.8	0.8353	4.9532
5	52.7	197.9	125.3	0.2978	1.7657	5	80.3	1385.8	733.1	1.0136	6.0106
10.3	52.7	197.5	125.1	0.3127	1.8543	10.8	82.4	1384.4	733.4	1.0786	6.3961
99.5	52.9	197.0	125.0	0.3331	1.9753	99.1	85.8	1382.0	733.9	1.1795	6.9944
754	53.0	195.7	124.3	0.3370	1.9985	738	86.5	1379.2	732.8	1.1936	7.0778
1.02 x10 ⁻⁴	53.5	499.0	276.2	0.1364	0.8086	1 x10 ⁻⁴	78.1	1591.8	834.9	0.8381	4.9696
1.012x10 ⁻³	53.5	498.8	276.2	0.1375	0.8156	.99x10 ⁻³	78.1	1591.9	835.0	0.8390	4.9753
1.025x10 ⁻²	53.7	499.0	276.3	0.1460	0.8655	1.05x10 ⁻²	78.4	1591.9	835.2	0.8462	5.0179
0.1115	54.2	498.5	276.3	0.1910	1.1326	0.1005	79.9	1591.5	835.7	0.8810	5.2242
0.504	55.2	497.2	276.2	0.2709	1.6064	0.5135	82.9	1590.3	836.6	0.9702	5.7534
1	55.8	497.0	276.4	0.3192	1.8929	1.025	84.7	1589.5	837.1	1.0370	6.1491
4.99	56.9	495.6	276.2	0.4162	2.4679	5	90.7	1586.8	838.8	1.2271	7.2766
10.1	57.2	495.1	276.1	0.4411	2.6158	10.6	93.0	1585.2	839.1	1.2993	7.7051
100.3	57.3	494.7	276.0	0.4762	2.8237	100	97.6	1582.0	839.8	1.4218	8.4314
736	56.6	491.3	273.9	0.4793	2.8422	737	98.4	1579.4	838.9	1.4408	8.5442
.997 x10 ⁻⁴	54.5	793.2	423.8	0.2476	1.4683	1.86 x10 ⁻⁴	90.4	1794.9	942.6	1.0798	6.4031
1.03x10 ⁻³	54.4	793.4	423.9	0.2488	1.4757	.964x10 ⁻³	90.8	1795.1	942.9	1.0807	6.4083
1x10 ⁻²	54.7	793.4	424.0	0.2572	1.5250	1.065x10 ⁻²	91.8	1795.1	943.5	1.0876	6.4496
0.105	55.5	792.7	424.1	0.2960	1.7554	0.104	93.9	1794.6	944.3	1.1238	6.6642
0.506	57.0	791.5	424.3	0.3825	2.2681	0.511	97.1	1793.4	945.3	1.2141	7.1996
0.999	58.0	790.9	424.5	0.4382	2.5986	1	99.6	1792.4	946.0	1.2816	7.6001
5.02	60.3	788.7	424.5	0.5660	3.3566	4.98	107.1	1788.5	947.8	1.4882	8.8253
10.7	60.9	788.5	424.7	0.6045	3.5849	10.25	109.8	1785.6	947.7	1.5668	9.2912
99.4	62.2	785.9	424.0	0.6554	3.8866	100.2	110.1	1790.7	950.4	1.6886	10.0136
740	62.1	783.3	422.7	0.6610	3.9197	750	111.2	1788.8	950.0	1.7134	10.1603
1.01 x10 ⁻⁴	59.6	1091.3	575.5	0.4115	2.4402						
.997x10 ⁻³	59.8	1091.7	575.7	0.4128	2.4480						
1.09x10 ⁻²	60.0	1091.7	575.8	0.4208	2.4956						
0.0984	61.0	1091.3	576.1	0.4562	2.7050						
0.506	63.2	1089.9	576.6	0.5458	3.2364						
1	64.5	1089.2	576.9	0.6068	3.5983						
5.03	68.2	1086.9	577.5	0.7631	4.5250						
11.1	69.7	1085.6	577.7	0.8162	4.8399						
99.8	71.8	1083.6	577.7	0.8890	5.2717						
756	72.2	1080.8	576.5	0.8957	5.3114						

Table 13. Effective thermal conductivity of Cerachrome™ at nominal density of 12 lb/ft³

P (torr)	T_cold °F	T_hot °F	T_avg °F	k Btu-in hr-ft ² -°F	ρk Btu-in-lb hr-ft ⁵ -°F	P (torr)	T_cold °F	T_hot °F	T_avg °F	k Btu-in hr-ft ² -°F	ρk Btu-in-lb hr-ft ⁵ -°F
1.02 x10 ⁻⁴	55.2	198.7	126.9	0.0294	0.3525	1x10 ⁻³	63.5	1388.6	726.0	0.2187	2.6246
1x10 ⁻³	55.3	198.7	127.0	0.0303	0.3633	1.02x10 ⁻²	64.0	1389.6	726.8	0.2256	2.7075
1x10 ⁻²	55.4	198.9	127.2	0.0358	0.4291	0.1055	64.9	1390.2	727.5	0.2413	2.8959
0.1	55.7	198.7	127.2	0.0602	0.7222	0.509	66.4	1390.0	728.2	0.2773	3.3272
0.5	56.0	198.7	127.4	0.1040	1.2479	1	67.3	1389.7	728.5	0.3077	3.6919
1	55.9	198.9	127.4	0.1301	1.5615	4.98	71.0	1388.1	729.6	0.4147	4.9761
5	56.0	198.4	127.2	0.1937	2.3239	10.7	72.8	1387.2	730.0	0.4636	5.5629
10.3	56.1	197.8	126.9	0.2105	2.5254	99.5	76.1	1385.6	730.8	0.5544	6.6525
99.6	56.2	197.1	126.7	0.2414	2.8973	748	77.4	1383.6	730.5	0.5820	6.9840
746	56.2	194.2	125.2	0.2498	2.9972	1x10 ⁻³	63.5	1388.6	726.0	0.2187	2.6246
1x10 ⁻³	55.9	493.1	274.5	0.0480	0.5765	1.02x10 ⁻²	64.0	1389.6	726.8	0.2256	2.7075
1.005x10 ⁻²	56.0	493.4	274.7	0.0551	0.6615	0.1055	64.9	1390.2	727.5	0.2413	2.8959
0.101	56.2	493.9	275.0	0.0764	0.9173	0.509	66.4	1390.0	728.2	0.2773	3.3272
0.499	56.6	493.7	275.2	0.1158	1.3900	1	67.3	1389.7	728.5	0.3077	3.6919
1	57.4	493.5	275.5	0.1460	1.7525	4.98	71.0	1388.1	729.6	0.4147	4.9761
4.99	58.6	493.1	275.8	0.2247	2.6960	10.7	72.8	1387.2	730.0	0.4636	5.5629
10.2	58.9	492.6	275.7	0.2493	2.9919	99.5	76.1	1385.6	730.8	0.5544	6.6525
101.2	59.2	492.0	275.6	0.2933	3.5190	748	77.4	1383.6	730.5	0.5820	6.9840
746	59.0	490.6	274.8	0.3055	3.6661	1x10 ⁻³	68.7	1590.1	829.4	0.2854	3.4245
1x10 ⁻³	56.9	791.5	424.2	0.0870	1.0442	1.015x10 ⁻²	69.1	1590.3	829.7	0.2899	3.4793
1.01x10 ⁻²	57.1	791.8	424.4	0.0952	1.1424	0.104	70.0	1590.3	830.2	0.3045	3.6538
0.101	57.7	792.0	424.9	0.1127	1.3525	0.501	71.3	1589.7	830.5	0.3396	4.0753
0.5	58.6	791.6	425.1	0.1512	1.8146	1	78.5	1588.1	833.3	0.3707	4.4488
1	59.2	791.2	425.2	0.1818	2.1812	4.98	83.3	1586.2	834.8	0.4820	5.7838
5	61.0	790.4	425.7	0.2728	3.2736	10.4	85.3	1585.2	835.2	0.5338	6.4055
10	61.6	790.2	425.9	0.3054	3.6646	100.4	89.9	1583.0	836.4	0.6406	7.6875
99.3	62.9	789.7	426.3	0.3637	4.3642	747	91.6	1580.7	836.2	0.6729	8.0747
746	63.3	787.6	425.5	0.3802	4.5625	1x10 ⁻³	79.5	1789.0	934.3	0.3632	4.3587
1x10 ⁻³	60.5	1092.6	576.5	0.1459	1.7506	1.025x10 ⁻²	80.0	1789.7	934.8	0.3676	4.4111
1x10 ⁻²	60.7	1092.8	576.8	0.1512	1.8149	0.105	81.3	1790.0	935.7	0.3828	4.5942
0.105	61.2	1092.9	577.0	0.1665	1.9984	0.508	83.2	1789.5	936.3	0.4169	5.0024
0.521	62.3	1092.3	577.3	0.2058	2.4692	1	84.7	1789.0	936.8	0.4471	5.3657
1	63.1	1091.8	577.5	0.2351	2.8211	5	90.0	1786.7	938.3	0.5619	6.7434
5.02	66.0	1090.4	578.2	0.3344	4.0133	10.4	92.3	1785.3	938.8	0.6182	7.4184
10.7	67.1	1089.7	578.4	0.3766	4.5194	99.7	98.2	1782.1	940.1	0.7391	8.8698
99.6	69.2	1088.8	579.0	0.4495	5.3941	748	100.4	1779.1	939.8	0.7756	9.3077
748	69.5	1086.9	578.2	0.4711	5.6537						

Table 14. Effective thermal conductivity of multi-layer insulation configuration 1 at nominal density of 1.5 lb/ft³

P (torr)	T_cold °F	T_hot °F	T_avg °F	k Btu-in hr-ft ² -°F	ρk Btu-in-lb hr-ft ⁵ -°F	P (torr)	T_cold °F	T_hot °F	T_avg °F	k Btu-in hr-ft ² -°F	ρk Btu-in-lb hr-ft ⁵ -°F
.99x10 ⁻³	51.2	201.1	126.1	0.0568	0.0847	1x10 ⁻⁴	62.8	1389.9	726.4	0.1291	0.1923
1.02x10 ⁻²	51.2	201.3	126.2	0.0782	0.1165	1.015x10 ⁻³	63.0	1390.1	726.6	0.1318	0.1963
0.101	51.6	199.1	125.4	0.1589	0.2368	1.045x10 ⁻²	63.4	1390.0	726.7	0.1498	0.2231
0.514	52.1	198.8	125.4	0.2439	0.3634	0.099	64.9	1389.5	727.2	0.2331	0.3473
1	52.3	199.6	125.9	0.2711	0.4040	0.503	67.5	1388.0	727.8	0.3535	0.5268
4.99	52.5	199.6	126.1	0.3066	0.4568	1	68.9	1387.3	728.1	0.4073	0.6069
10.3	52.6	198.7	125.6	0.3140	0.4679	4.99	72.1	1385.8	728.9	0.5018	0.7477
100	52.7	198.0	125.4	0.3228	0.4810	10.4	73.1	1384.3	728.7	0.5243	0.7812
750	52.7	197.1	124.9	0.3249	0.4841	99.7	74.9	1382.2	728.6	0.5575	0.8307
1x10 ⁻⁴	54.2	796.6	424.9	0.0818	0.1218	750	75.4	1380.1	727.7	0.5694	0.8485
.991x10 ⁻³	54.4	796.8	425.4	0.0848	0.1264	1.04x10 ⁻⁴	74.0	1794.9	934.5	0.2051	0.3056
1.02x10 ⁻²	54.6	796.3	427.5	0.1024	0.1526	1.11x10 ⁻³	74.2	1795.0	934.6	0.2079	0.3097
0.102	55.6	796.1	437.8	0.1831	0.2728	1.05x10 ⁻²	74.5	1794.9	934.7	0.2254	0.3358
0.501	57.1	795.3	450.8	0.2862	0.4265	0.1006	76.2	1794.1	935.2	0.2975	0.4433
1.01	57.8	794.5	455.9	0.3287	0.4898	0.51	78.9	1792.5	935.7	0.4074	0.6070
5.01	59.3	793.4	463.7	0.3925	0.5849	1	80.8	1791.7	936.2	0.4622	0.6886
10.4	59.7	792.4	464.8	0.4056	0.6043	5.01	85.9	1789.4	937.6	0.5829	0.8686
99.8	60.2	792.4	467.2	0.4240	0.6318	10.2	87.7	1788.1	937.9	0.6198	0.9234
748	60.4	788.8	466.0	0.4281	0.6379	100	91.3	1784.9	938.1	0.6816	1.0156
						752	92.3	1781.5	936.9	0.7024	1.0465

Table 15. Effective thermal conductivity of multi-layer insulation configuration 2 at nominal density of 3 lb/ft³

P (torr)	T_cold °F	T_hot °F	T_avg °F	k Btu-in hr-ft ² -°F	ρk Btu-in-lb hr-ft ⁵ -°F	P (torr)	T_cold °F	T_hot °F	T_avg °F	k Btu-in hr-ft ² -°F	ρk Btu-in-lb hr-ft ⁵ -°F
1.01x10 ⁻⁴	52.5	200.8	126.6	0.0427	0.1282	.999x10 ⁻⁴	59.2	1392.5	725.8	0.0896	0.2688
1.006x10 ⁻³	52.3	200.3	126.3	0.0455	0.1364	1.005x10 ⁻³	59.3	1392.5	725.9	0.0914	0.2743
1.01x10 ⁻²	52.2	200.0	126.1	0.0610	0.1831	1.04x10 ⁻²	59.7	1392.4	726.1	0.1040	0.3120
0.101	52.3	199.7	126.0	0.1203	0.3608	0.1	61.6	1391.6	726.6	0.1511	0.4533
0.5	52.5	199.4	125.9	0.1962	0.5887	0.505	64.5	1390.3	727.4	0.2323	0.6969
1.03	52.5	199.2	125.8	0.2276	0.6829	0.993	66.1	1389.9	728.0	0.2763	0.8288
4.98	52.6	198.8	125.7	0.2722	0.8167	5.01	69.9	1387.7	728.8	0.3821	1.1464
10.6	52.8	198.3	125.5	0.2828	0.8484	10.7	71.2	1386.4	728.8	0.4181	1.2543
99.8	52.8	198.0	125.4	0.2977	0.8930	99.8	73.9	1384.0	729.0	0.4801	1.4404
751	52.6	196.7	124.7	0.3011	0.9033	752	74.2	1381.3	727.8	0.5010	1.5029
.993x10 ⁻⁴	52.9	793.8	423.4	0.0572	0.1717	1.1x10 ⁻⁴	66.4	1797.1	931.7	0.1220	0.3661
.99x10 ⁻³	53.1	793.9	423.5	0.0595	0.1786	1.005x10 ⁻³	66.5	1797.3	931.9	0.1236	0.3709
1.015x10 ⁻²	53.3	793.8	423.5	0.0727	0.2180	1.065x10 ⁻²	67.0	1797.4	932.2	0.1323	0.3970
0.102	54.4	792.9	423.6	0.1261	0.3782	0.1029	69.1	1796.9	933.0	0.1786	0.5359
0.505	55.9	792.2	424.0	0.2110	0.6329	0.51	72.9	1795.7	934.3	0.2538	0.7614
1.01	56.8	792.0	424.4	0.2527	0.7582	0.993	74.8	1794.9	934.9	0.2972	0.8915
5	58.5	790.6	424.5	0.3287	0.9862	4.99	80.2	1792.5	936.3	0.4207	1.2622
10.7	58.9	789.0	424.0	0.3483	1.0448	11	82.7	1790.7	936.7	0.4733	1.4198
99.4	59.7	787.1	423.4	0.3784	1.1351	108	87.3	1787.5	937.4	0.5717	1.7152
749	59.9	785.1	422.5	0.3870	1.1609	749	87.9	1783.7	935.8	0.6057	1.8170

Table 16. Effective thermal conductivity of multi-layer insulation configuration 3 at nominal density of 3 lb/ft³

P (torr)	T_cold °F	T_hot °F	T_avg °F	k Btu-in hr-ft ² -°F	ρk Btu-in-lb hr-ft ⁵ -°F	P (torr)	T_cold °F	T_hot °F	T_avg °F	k Btu-in hr-ft ² -°F	ρk Btu-in-lb hr-ft ⁵ -°F
1x10 ⁻⁴	51.6	200.0	125.8	0.0144	0.0428	1x10 ⁻⁴	57.0	1389.2	723.1	0.0578	0.1716
1.015x10 ⁻³	51.7	200.2	125.9	0.0146	0.0432	1.07x10 ⁻³	57.1	1389.7	723.4	0.0589	0.1749
1.025x10 ⁻²	51.8	200.4	126.1	0.0225	0.0669	1.05x10 ⁻²	57.4	1389.8	723.6	0.0659	0.1956
0.1015	52.0	200.1	126.1	0.0611	0.1814	0.1055	58.7	1389.5	724.1	0.0969	0.2877
0.4985	52.4	199.3	125.9	0.1246	0.3701	0.5235	61.2	1388.5	724.9	0.1730	0.5139
1	52.6	198.7	125.7	0.1562	0.4639	1	62.8	1388.0	725.4	0.2244	0.6665
4.99	52.7	198.5	125.6	0.2079	0.6173	5.02	67.4	1386.2	726.8	0.3733	1.1087
10.7	52.9	198.2	125.6	0.2185	0.6490	10.8	69.0	1385.2	727.1	0.4230	1.2562
99.7	53.1	197.5	125.3	0.2324	0.6901	99.95	71.5	1382.9	727.2	0.4842	1.4380
750	53.4	196.4	124.9	0.2365	0.7023	748	72.0	1380.3	726.2	0.4932	1.4649
1.01x10 ⁻⁴	53.2	792.8	423.0	0.0234	0.0695	1.55x10 ⁻⁴	63.9	1795.5	929.7	0.1041	0.3093
1.065x10 ⁻³	52.9	793.0	422.9	0.0254	0.0754	1.113x10 ⁻³	63.9	1795.8	929.9	0.1051	0.3123
1.02x10 ⁻²	53.1	792.9	423.0	0.0341	0.1014	1.04x10 ⁻²	64.4	1795.9	930.2	0.1103	0.3276
0.102	53.9	792.5	423.2	0.0683	0.2029	0.104	65.9	1795.6	930.8	0.1353	0.4019
5.12	55.3	791.4	423.4	0.1421	0.4220	0.506	68.7	1794.7	931.7	0.1954	0.5805
1	56.1	791.4	423.7	0.1883	0.5593	1.005	70.9	1794.0	932.4	0.2473	0.7344
5.015	57.9	789.7	423.8	0.2886	0.8572	5.03	77.9	1791.5	934.7	0.4261	1.2654
11.2	58.5	789.4	423.9	0.3149	0.9353	11	81.0	1789.8	935.4	0.5050	1.4998
99.6	59.4	786.4	422.9	0.3430	1.0186	100.05	85.9	1786.0	936.0	0.6157	1.8287
746	59.5	784.3	421.9	0.3497	1.0385	749	86.5	1781.2	933.8	0.6278	1.8647

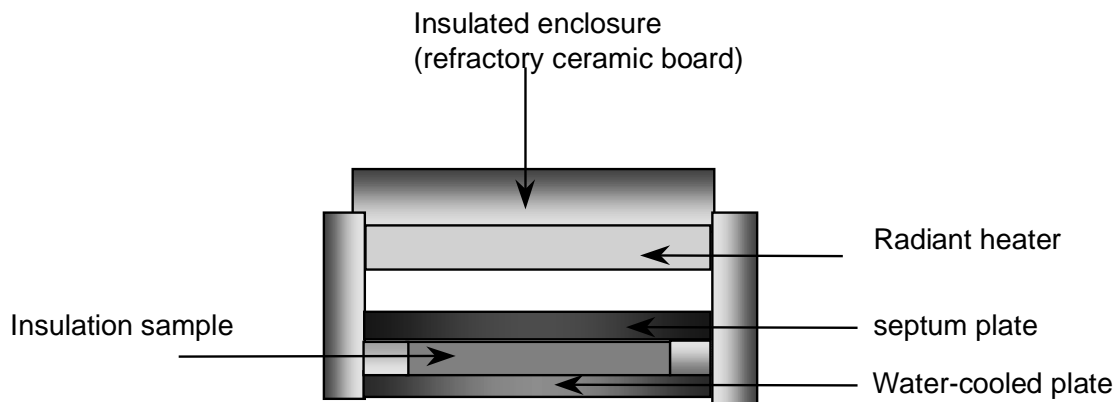


Figure 1. Schematic of the thermal conductivity apparatus

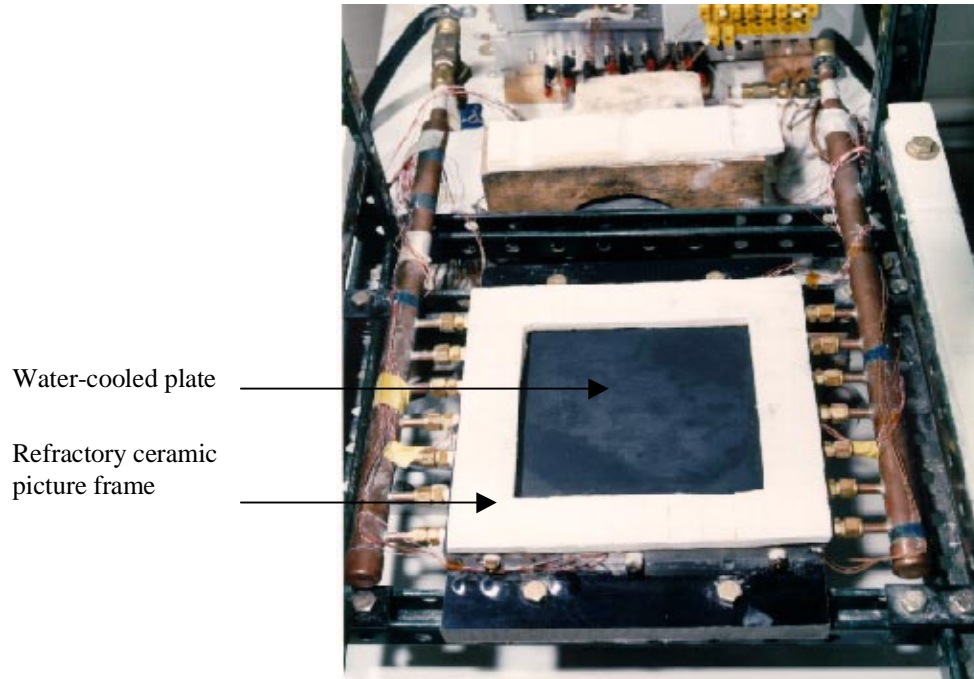


Figure 2. Photograph of thermal conductivity apparatus with picture frame set on the water-cooled plate

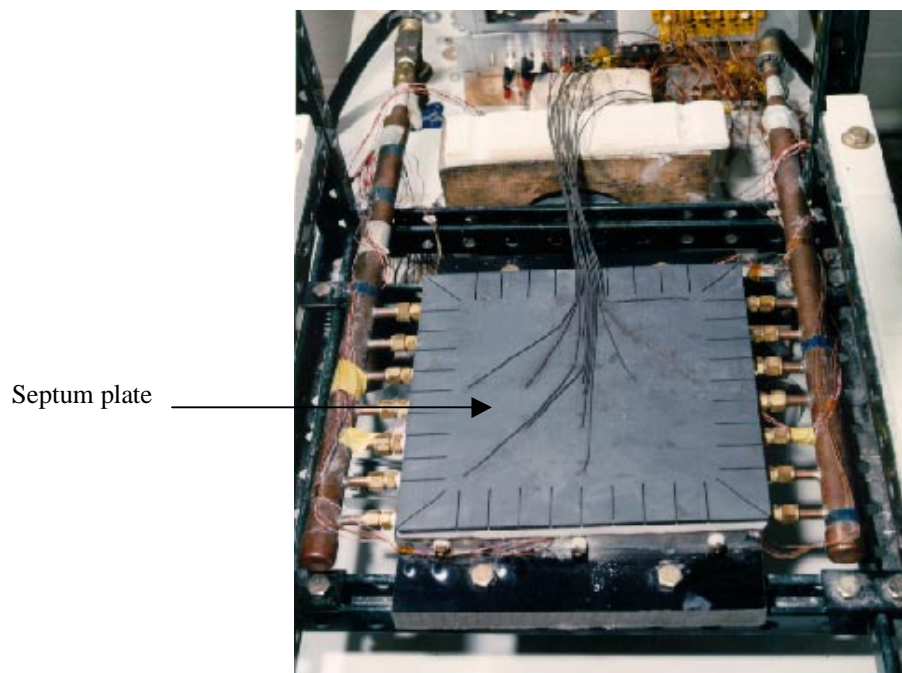


Figure 3. Photograph of thermal conductivity apparatus with septum plate set on the picture frame and insulation sample

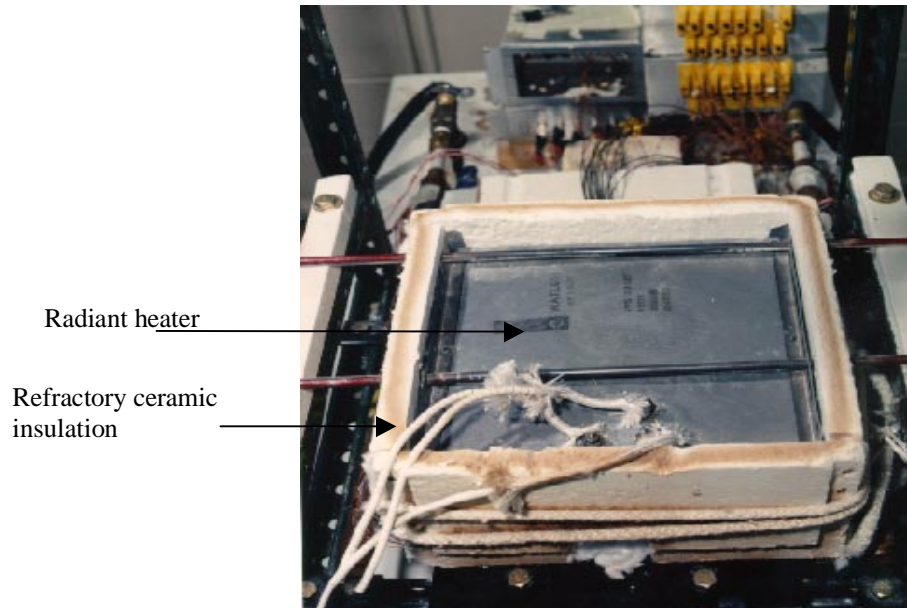


Figure 4. Photograph of radiant heater and insulation enclosure set on the thermal conductivity apparatus



Figure 5. Photograph of the thermal conductivity apparatus set in the vacuum chamber

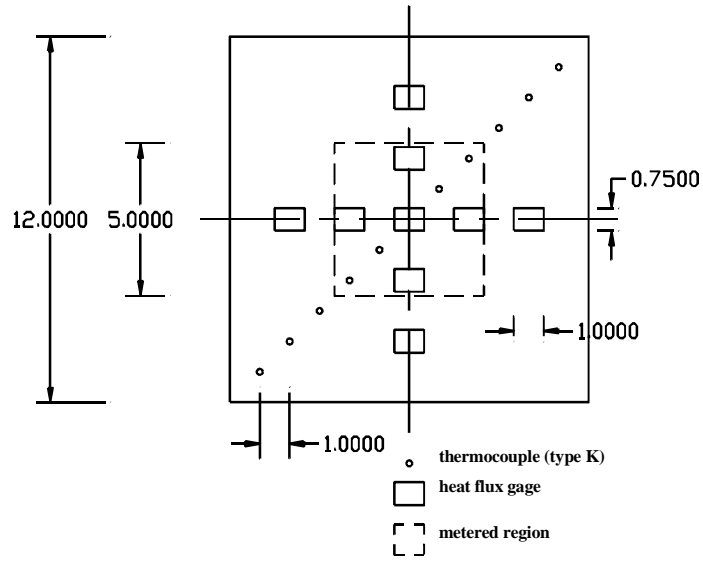


Figure 6. Instrumentation layout on water-cooled plate

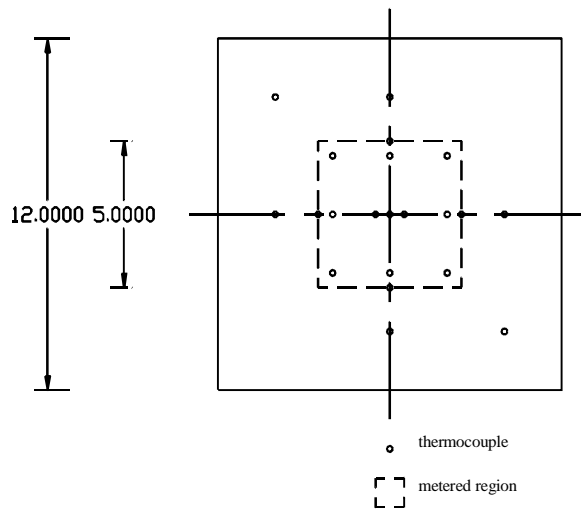


Figure 7. Instrumentation layout on septum plate

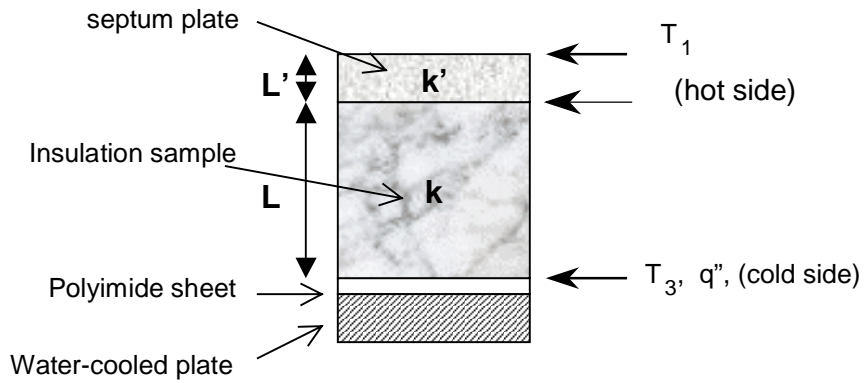


Figure 8. Schematic of 1-D set-up for calculation of effective thermal conductivity

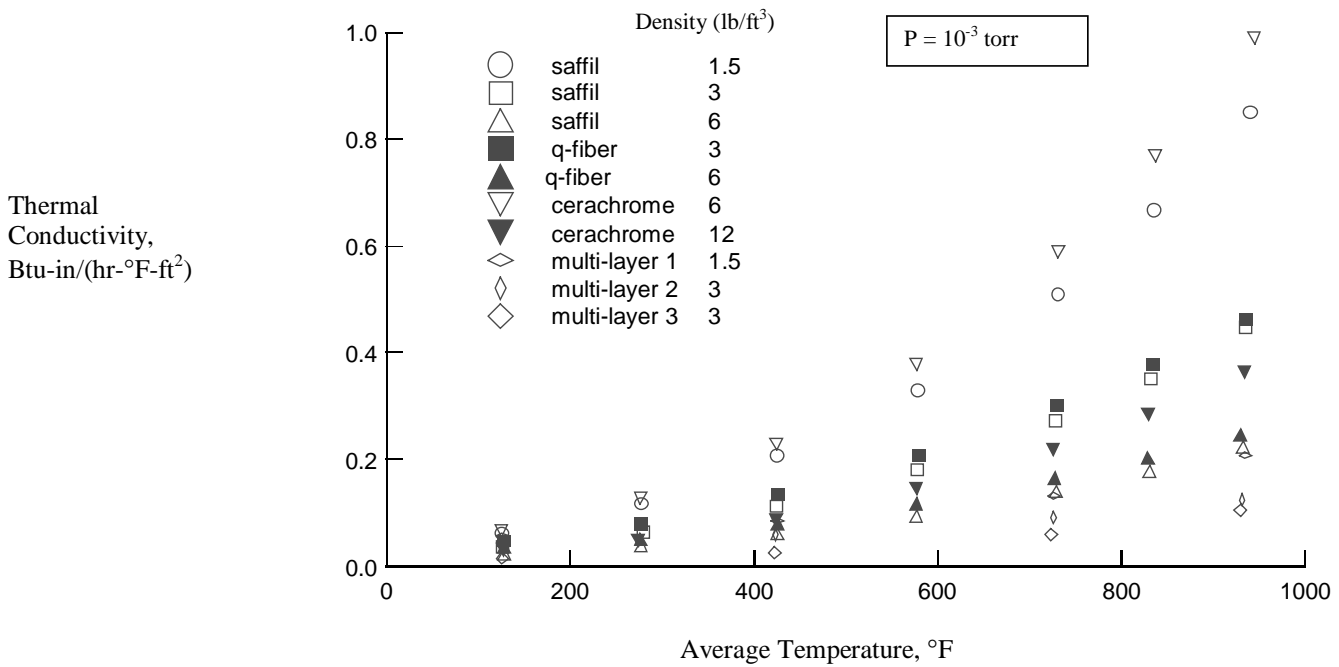


Figure 9. Variation of effective thermal conductivity of various samples with sample average temperature at different pressures

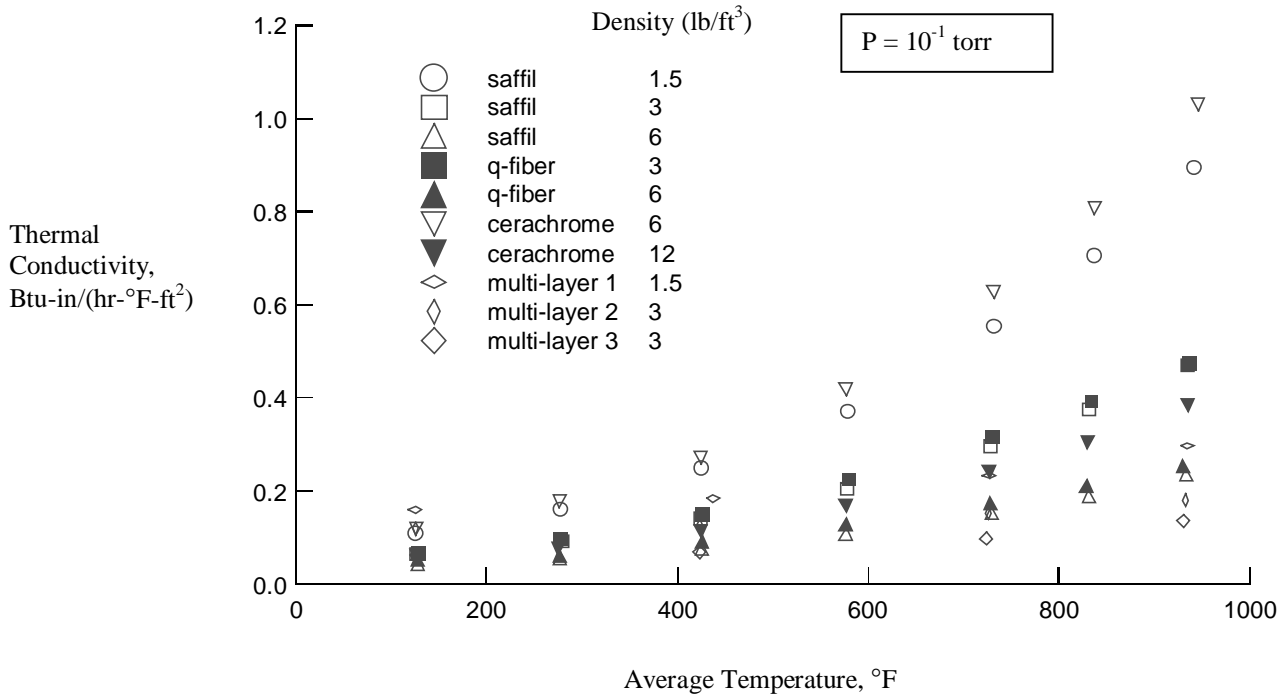


Figure 9. Continued.

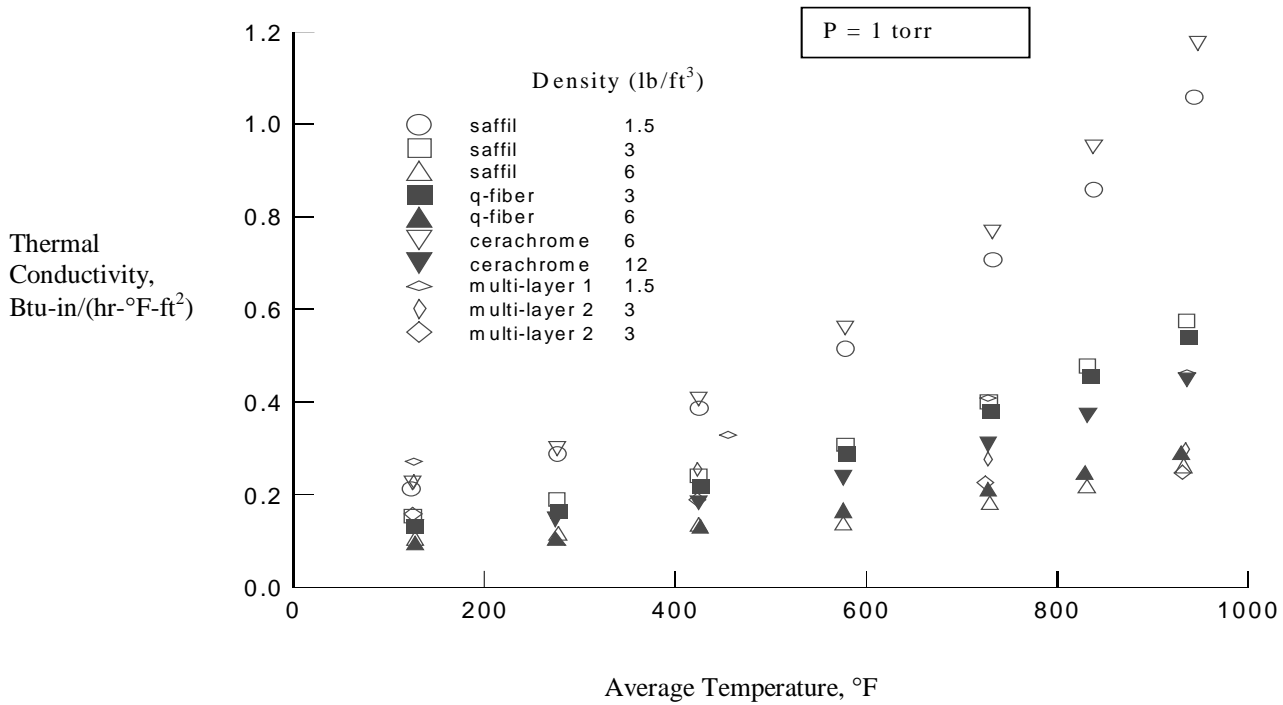


Figure 9. Continued.

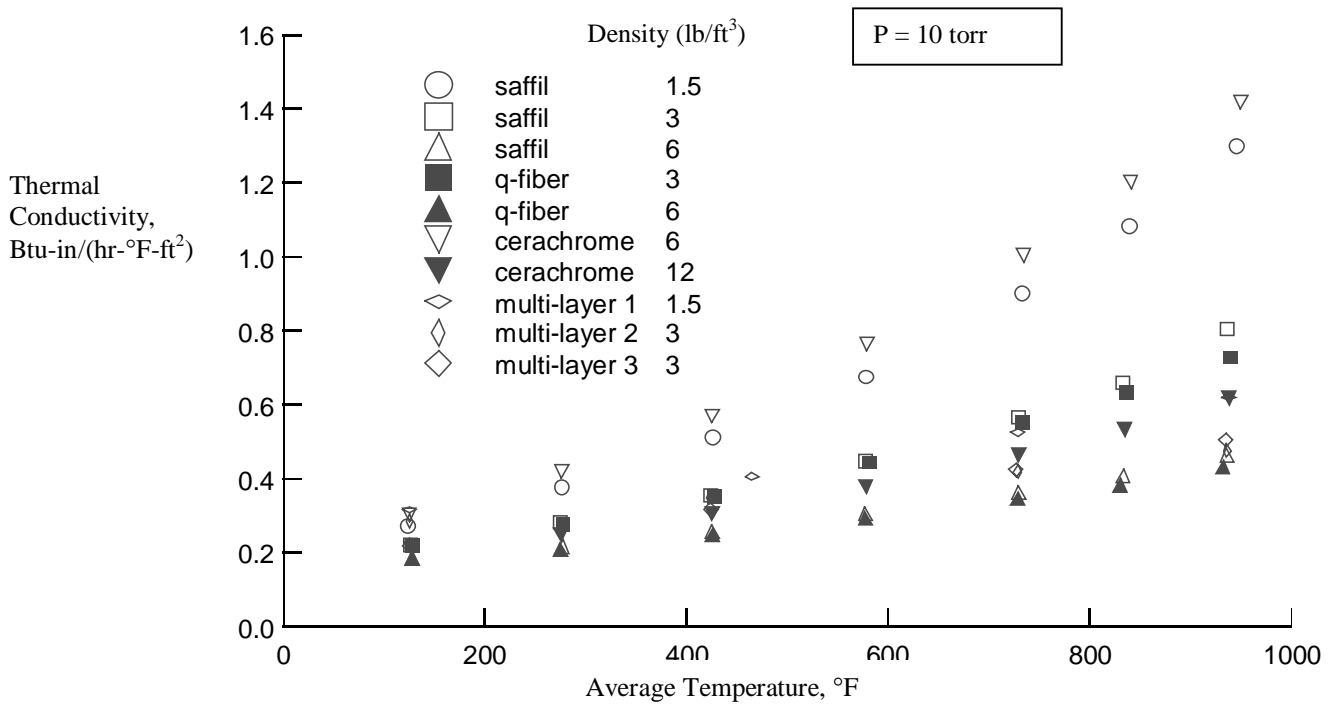


Figure 9. Continued.

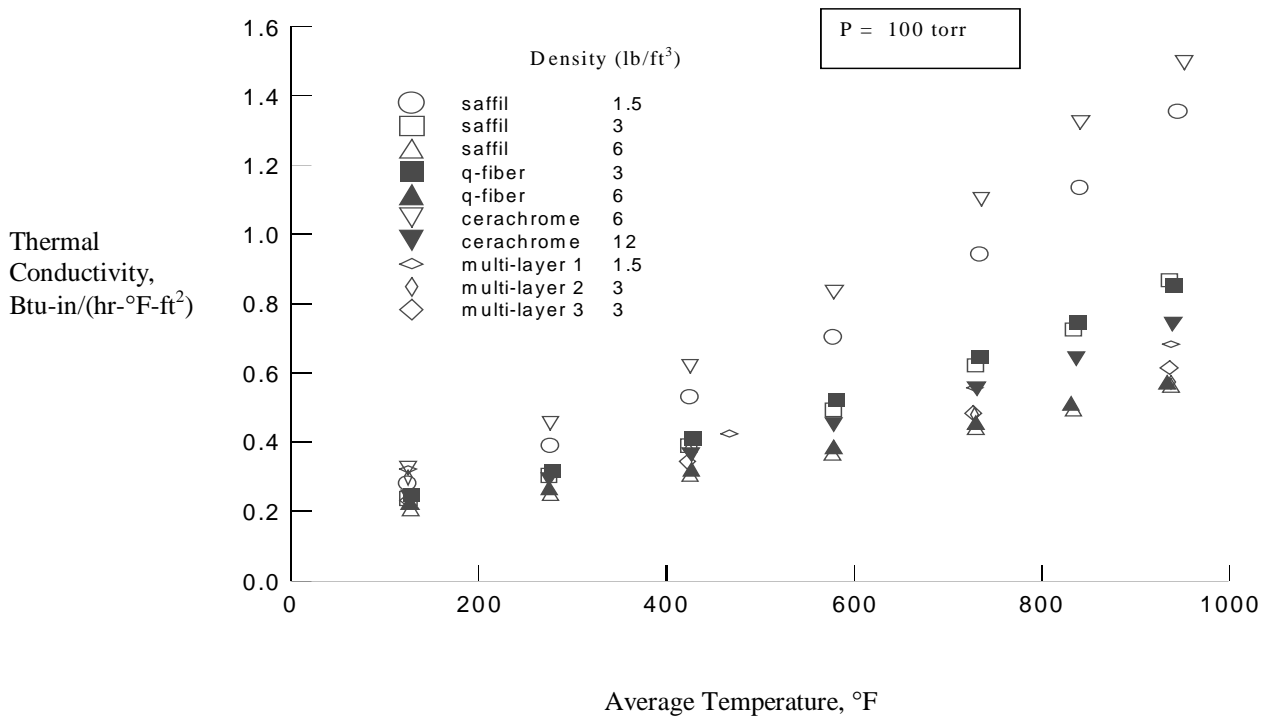


Figure 9. Concluded.

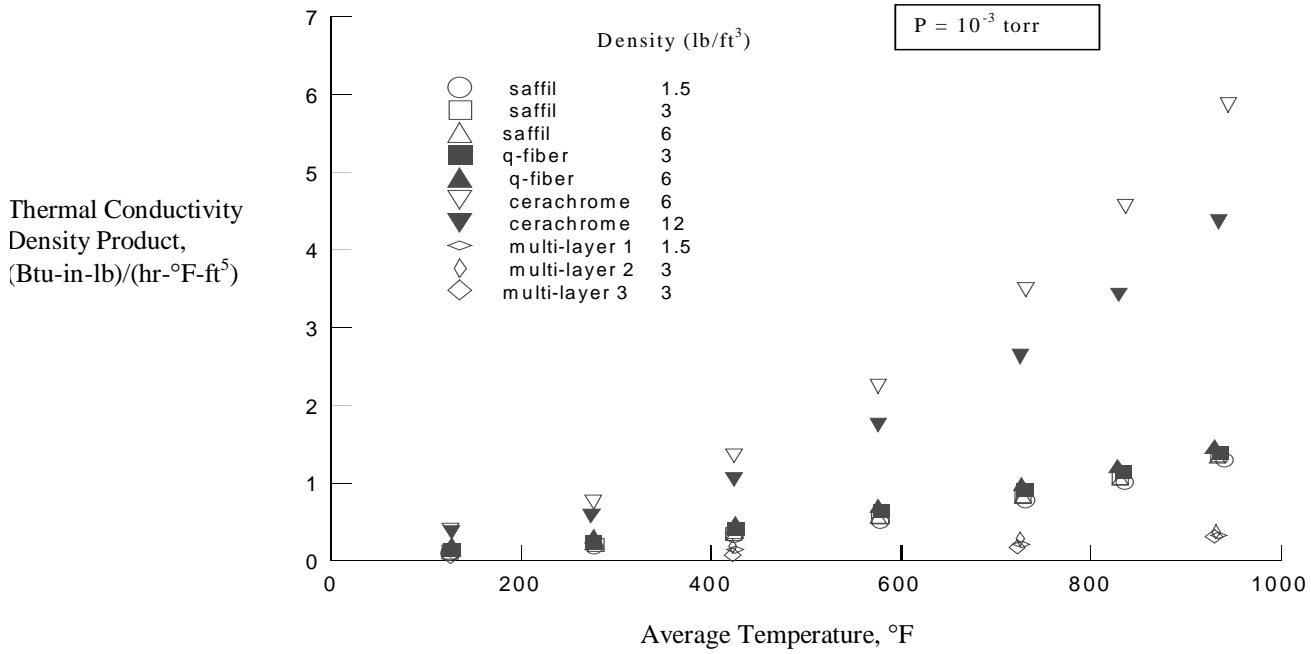


Figure 10. Variation of the product of effective thermal conductivity and density of various samples with sample average temperature at different pressures

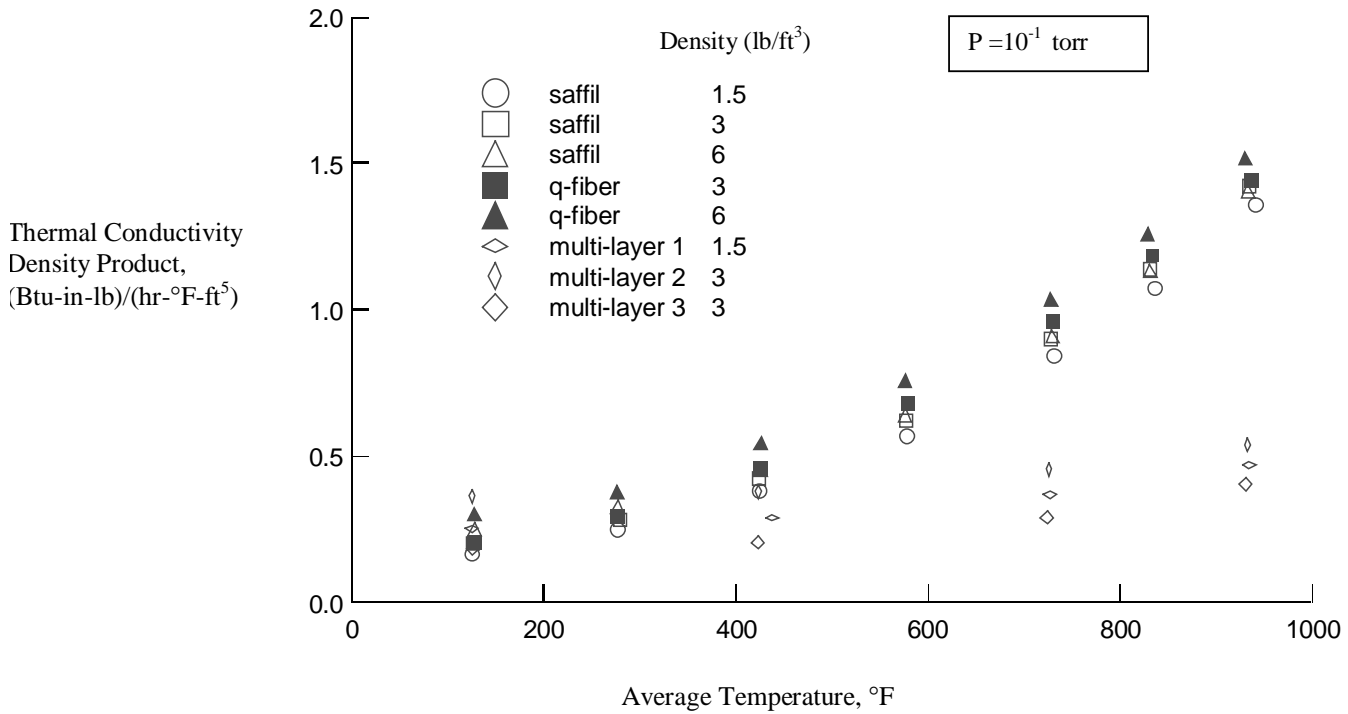


Figure 10. Continued.

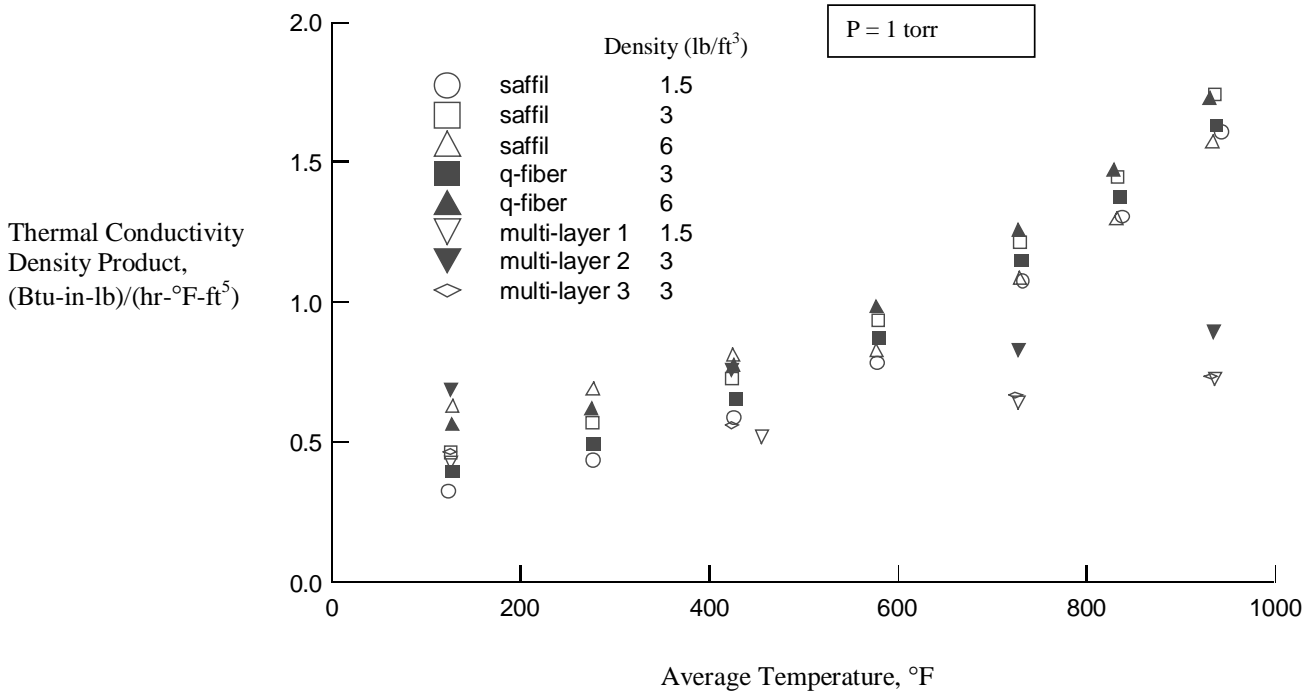


Figure 10. Continued.

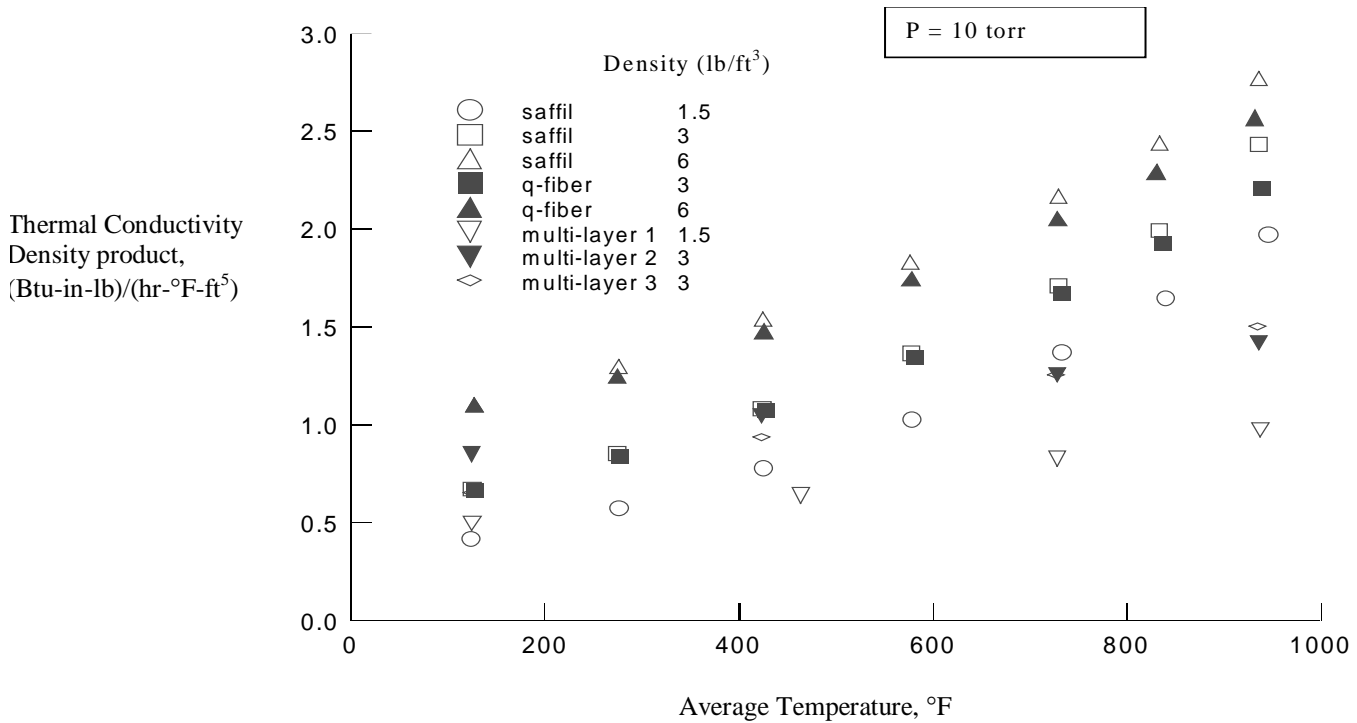


Figure 10. Continued.

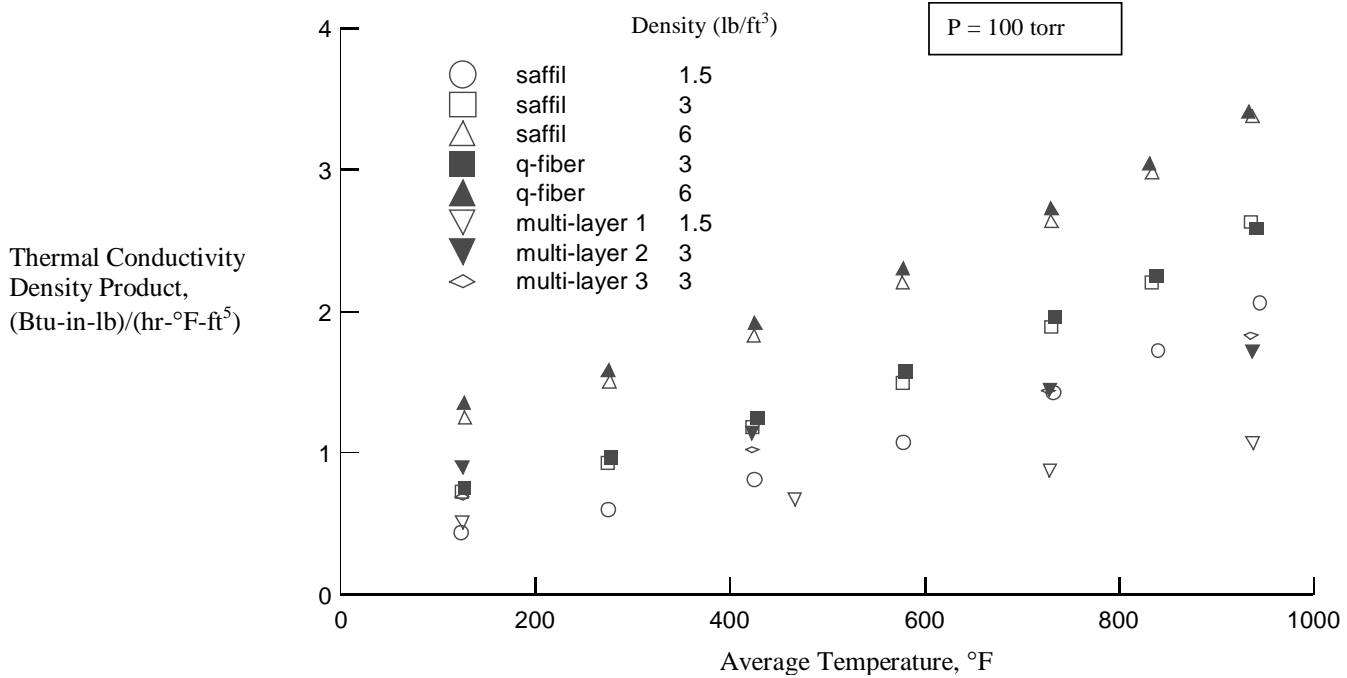


Figure 10. Concluded

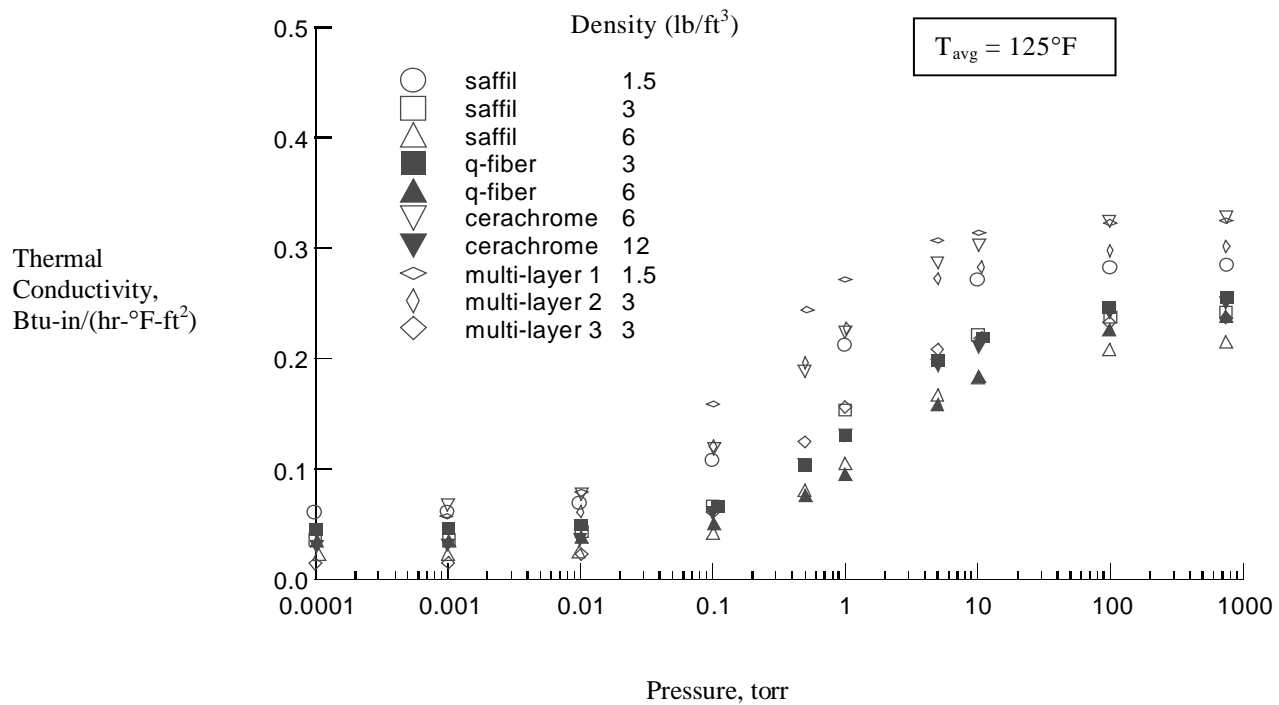


Figure 11. Variation of effective thermal conductivity of various samples with pressures at different sample average temperatures

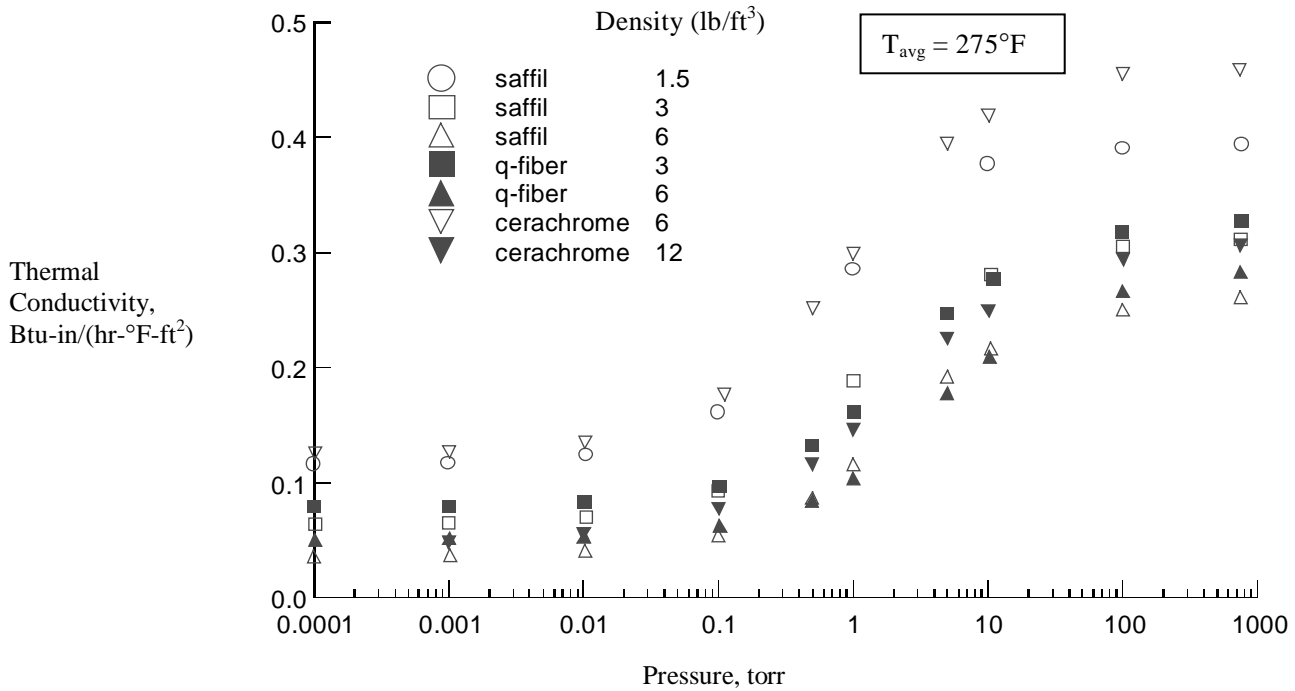


Figure 11. Continued.

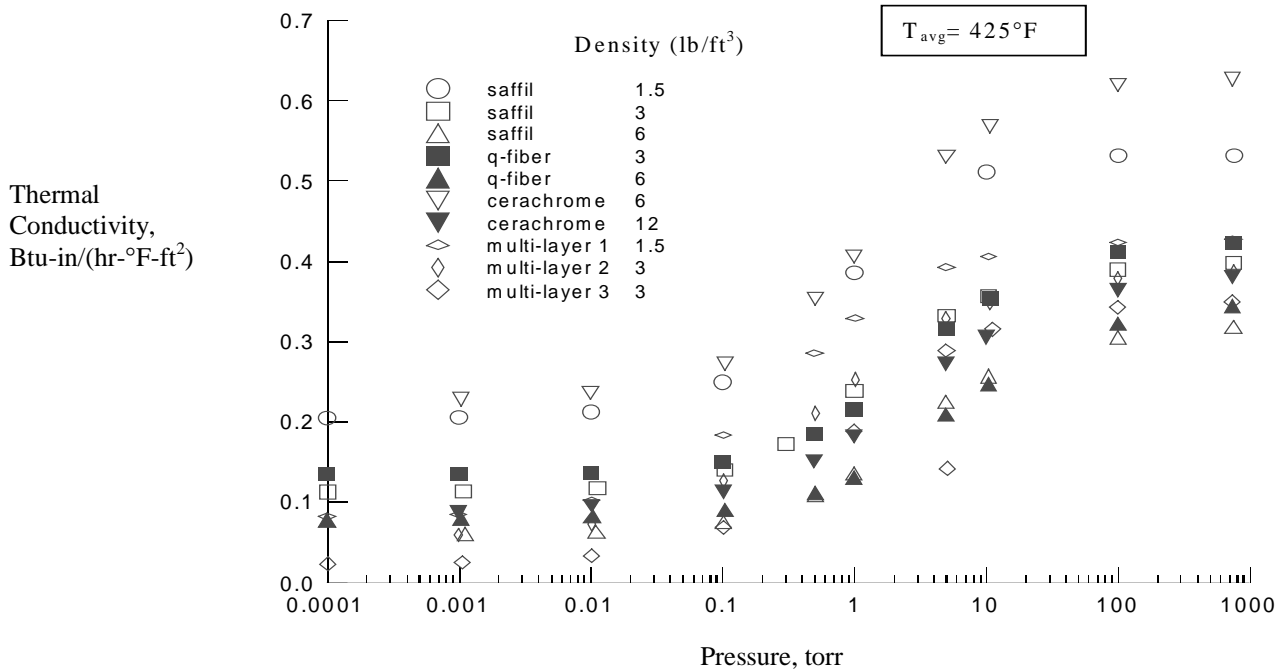


Figure 11. Continued

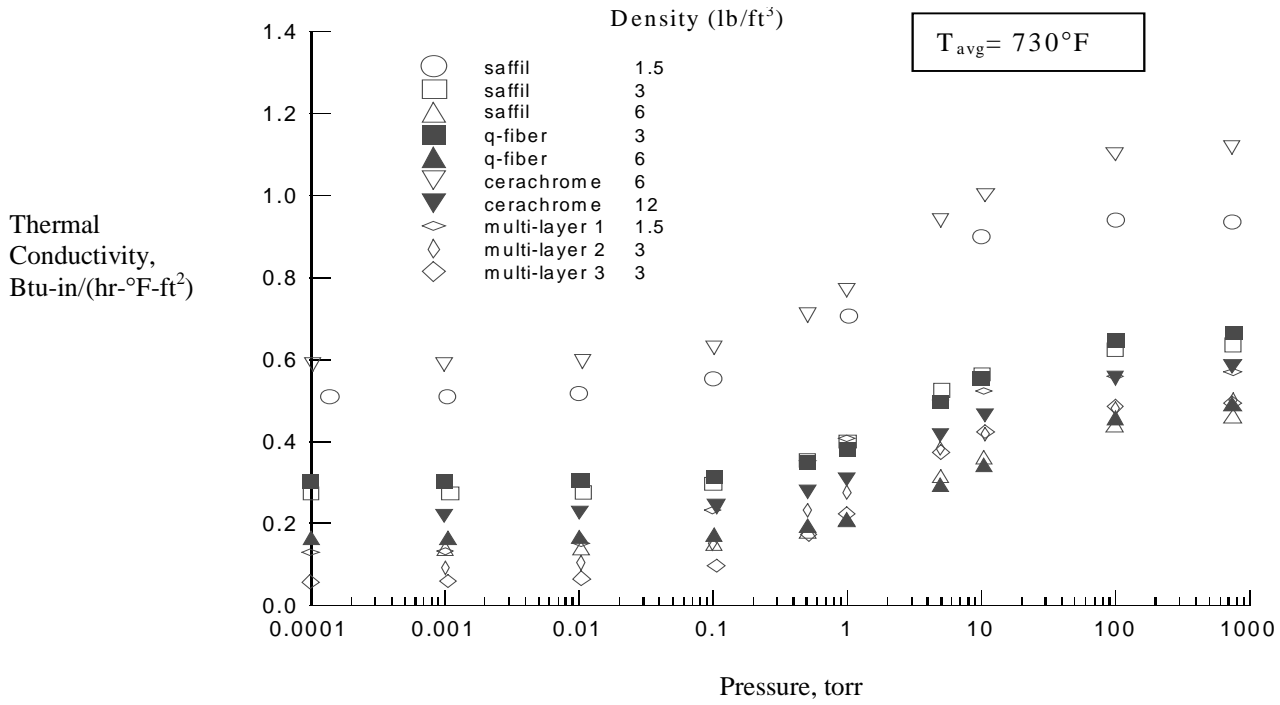


Figure 11. Continued

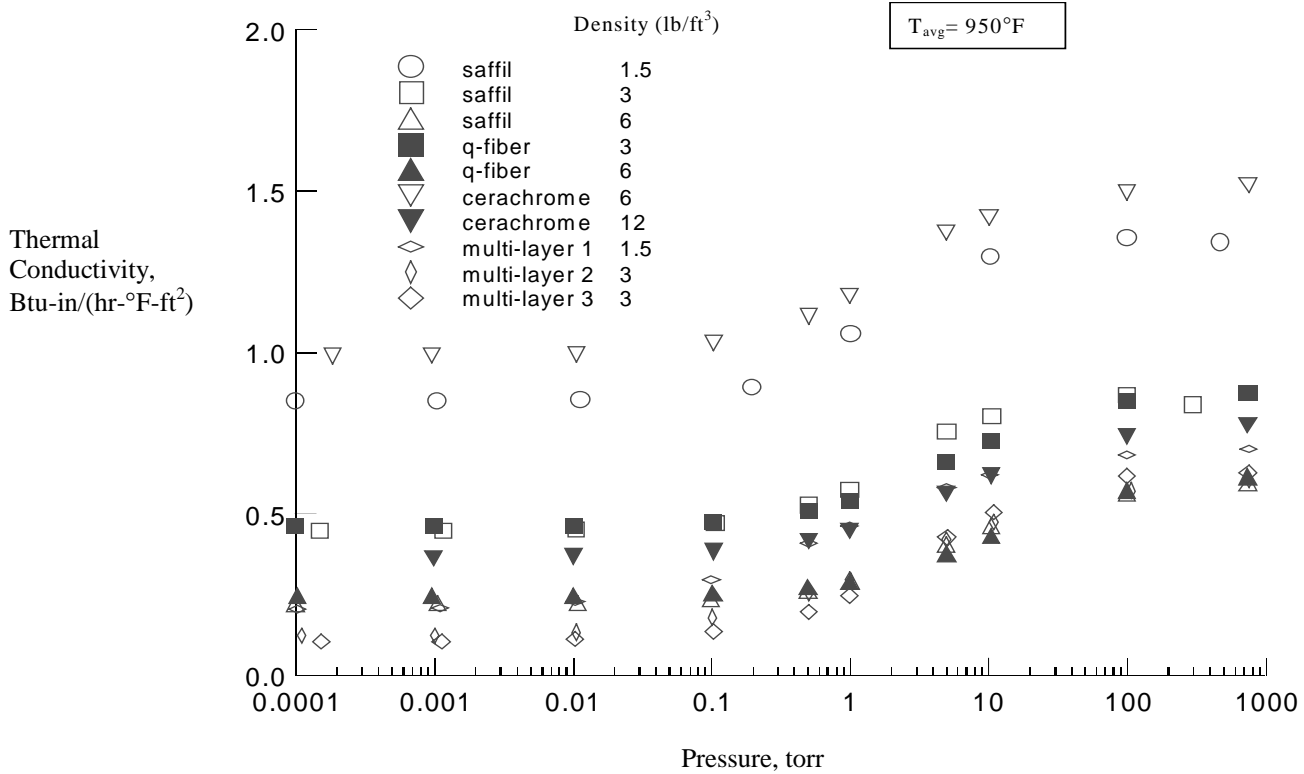


Figure 11. Concluded

REPORT DOCUMENTATION PAGE			Form Approved OMB No. 0704-0188
Public reporting burden for this collection of information is estimated to average 1 hour per response, including the time for reviewing instructions, searching existing data sources, gathering and maintaining the data needed, and completing and reviewing the collection of information. Send comments regarding this burden estimate or any other aspect of this collection of information, including suggestions for reducing this burden, to Washington Headquarters Services, Directorate for Information Operations and Reports, 1215 Jefferson Davis Highway, Suite 1204, Arlington, VA 22202-4302, and to the Office of Management and Budget, Paperwork Reduction Project (0704-0188), Washington, DC 20503.			
1. AGENCY USE ONLY (Leave blank)	2. REPORT DATE February 1999	3. REPORT TYPE AND DATES COVERED Technical Memorandum	
4. TITLE AND SUBTITLE Effective Thermal Conductivity of High Temperature Insulations for Reusable Launch Vehicles		5. FUNDING NUMBERS 242-33-03-29	
6. AUTHOR(S) Kamran Daryabeigi			
7. PERFORMING ORGANIZATION NAME(S) AND ADDRESS(ES) NASA Langley Research Center Hampton, VA 23681-2199		8. PERFORMING ORGANIZATION REPORT NUMBER L-17808	
9. SPONSORING/MONITORING AGENCY NAME(S) AND ADDRESS(ES) National Aeronautics and Space Administration Washington, DC 20546-0001		10. SPONSORING/MONITORING AGENCY REPORT NUMBER NASA/TM-1999-208972	
11. SUPPLEMENTARY NOTES			
12a. DISTRIBUTION/AVAILABILITY STATEMENT Unclassified-Unlimited Subject Category 34 Distribution: Standard Availability: NASA CASI (301) 621-0390		12b. DISTRIBUTION CODE	
13. ABSTRACT (Maximum 200 words) An experimental apparatus was designed to measure the effective thermal conductivity of various high temperature insulations subject to large temperature gradients representative of typical launch vehicle re-entry aerodynamic heating conditions. The insulation sample cold side was maintained around room temperature, while the hot side was heated to temperatures as high as 1800 degrees Fahrenheit. The environmental pressure was varied from 0.0001 to 760 torr. All the measurements were performed in a dry gaseous nitrogen environment. The effective thermal conductivity of Saffil, Q-Fiber felt, Cerachrome, and three multi-layer insulation configurations were measured.			
14. SUBJECT TERMS Thermal conductivity; Fibrous insulation, Multi-layer insulation		15. NUMBER OF PAGES 35	
		16. PRICE CODE A03	
17. SECURITY CLASSIFICATION OF REPORT Unclassified	18. SECURITY CLASSIFICATION OF THIS PAGE Unclassified	19. SECURITY CLASSIFICATION OF ABSTRACT Unclassified	20. LIMITATION OF ABSTRACT UL